A Study of the Spectral and Redox Properties and Covalent Flavinylation of the Flavoprotein Component of *p*-Cresol Methylhydroxylase Reconstituted with FAD Analogues†

Igor Efimov and William S. McIntire*

Molecular Biology Division, Department of Veterans Affairs Medical Center, San Francisco, California 94121, and Department of Biochemistry and Biophysics, University of California, San Francisco, California 94143

Received March 31, 2004; Revised Manuscript Received May 21, 2004

ABSTRACT: The spectral and redox properties are described for the wild-type and Y384F mutant forms of the flavoprotein component (PchF) of flavocytochrome, *p*-cresol methylhydroxylase (PCMH), and cytochrome-free PchF that harbor FAD analogues. The analogues are iso-FAD (8-demethyl-6-methyl-FAD), 6-amino-FAD (6-NH_2-FAD), 6-bromo-FAD (6-Br-FAD), 8-nor-8-chloro-FAD (8-Cl-FAD), and 5-deaza-5-carba-FAD (5-deaza-FAD). All of the analogues bound noncovalently and stoichiometrically to cytochrome-free apo-PchF, and the resulting holoproteins had high affinity for the cytochrome subunit, PchC. Noncovalently bound FAD, 6-Br-FAD, or 6-NH_2-FAD can be induced to bind covalently by exposing holo-PchF to PchC. The rate of this process and the redox potential of the noncovalently bound flavin may be correlated. In addition, the redox potential of each FAD analogue was higher when it was covalently bound than when noncovalently bound to PchF. Furthermore, the potential of a covalently bound or noncovalently bound FAD analogue increased on association of the corresponding holo-PchF with PchC, and the activity increased as the flavin's redox potential increased. It was discovered also that 4-hydroxybenzaldehyde, the final *p*-cresol oxidation product, is an efficient competitive inhibitor for substrate oxidation by PchF since it binds tightly to this protein when the flavin is oxidized, although it binds more loosely to the enzyme with reduced flavin. Finally, the energies of the charge-transfer bands for the interaction of bound flavin analogues with 4-Br-phenol (a substrate mimic) increased as the potential decreases, although a simple global correlation was not seen. This is the case because the energy is also a function of the redox properties of the bound mimic. The implications of these findings to covalent flavinylation and catalysis are discussed.

p-Cresol methylhydroxylase (PCMH)[1] is an $\alpha_2\beta_2$ flavocytochrome from *Pseudomonas putida*. PCMH oxidizes *p*-cresol (4-methylphenol) to 4-hydroxybenzyl alcohol, which is oxidized further by the enzyme to 4-hydroxybenzaldehyde. A *c*-type cytochrome subunit (β or PchC; 10 kDa) associates with each α flavoprotein subunit (PchF) of an intimately associated α_2 homodimer (*1*). FAD is attached covalently to the 58 kDa PchF subunit through a bond between the 8α-carbon of the flavin's isoalloxazine ring and phenolic oxygen of Tyr384 (Figure 1) (*2*). Our *Escherichia coli* expression system provides PchC-free PchF containing FAD noncovalently bound (PchF{FAD}^{NC})[2] (*3*). Only after PchF-{FAD}^{NC} is exposed to PchC does the flavin attach covalently to yield natural PCMH (*4*) (Figure 1). This system is unique among covalent flavoproteins since it is the only one for which covalent flavinylation can be studied directly in vitro (*3*, *4*). Since isoelectric focusing (IEF) of PCMH separates easily PchF with covalently bound FAD (PchF-{FAD}^{C}) from PchC (*5*), it has been possible to study the properties of PCMH, PchF{FAD}^{NC}, and PchF{FAD}^{C}.

Our prior work allows us to formulate a mechanism for covalent flavinylation: First, FAD binds rapidly to apo-PchF to give PchF{FAD}^{NC}. This results in an increase in the 2-electron midpoint potential ($E_{m,7}$, SHE)[3] from −219 mV for free FAD to −16 mV for PchF{FAD}^{NC}. Next, PchC

† This work was supported by the Department of Veterans Affairs and NIH Grant GM-61651.

* To whom correspondence should be addressed at the Department of Veterans Affairs Medical Center. Tel: 415-387-1431. Fax: 415-650-6959. E-mail: wsm@itsa.ucsf.edu.

[1] Abbreviations: 6-NH_2-FAD, 6-amino-FAD; 6-NH_2-Rbf, 6-amino-riboflavin; 6-Br-FAD, 6-bromo-FAD; 4-Br-phenol, 4-bromophenol; 6-Br-Rbf, 6-bromoriboflavin; 8-Cl-FAD, 8-nor-8-chloro-FAD; 8-Cl-Rbf, 8-nor-8-chlororiboflavin; 5-deaza-FAD, 5-deaza-5-carba-FAD; 5-deaza-Rbf, 5-deaza-5-carbariboflavin; CT, charge transfer; DCIP, 2,6-dichlorophenolindophenol; E^A, electron affinity; E_{CT}, energy corresponding to the wavelength for the maximum absorbance of the CT complex between protein-bound flavin and 4-bromophenol; $E_{m,7}$, midpoint potentials (relative to the standard hydrogen electrode, SHE) measured at pH 7.0 and 25 °C; iso-FAD, 8-demethyl-6-methyl-FAD; I^D, ionization potential; iso-Rbf, isoriboflavin or 8-demethyl-6-methyl-riboflavin; PchC, the *c*-type cytochrome subunit of PCMH; PchF, the flavoprotein subunit of PCMH; {X}^{C}, where X is either FAD, 6-Br-FAD, or 6-NH_2-FAD covalently bound to various forms of PchF or PCMH, e.g., PchF{6-Br-FAD}^{C}; {X}^{NC}, where X is either FAD, 6-NH_2-FAD, 6-Br-FAD, 8-Cl-FAD, 5-deaza-FAD, or isoFAD noncovalently bound to various forms of PchF or PCMH, e.g., PCMH{8-Cl-FAD}^{NC}; PCMH, *p*-cresol methylhydroxylase; PES, phenazine ethosulfate; Rbf, riboflavin.

[2] The NC and C superscripts designate FAD noncovalently bound and covalently bound to PchF, respectively.

[3] All potentials reported in this paper are relative to the standard hydrogen electrode (SHE).

10.1021/bi049375d CCC: $27.50
Published on Web 07/22/2004

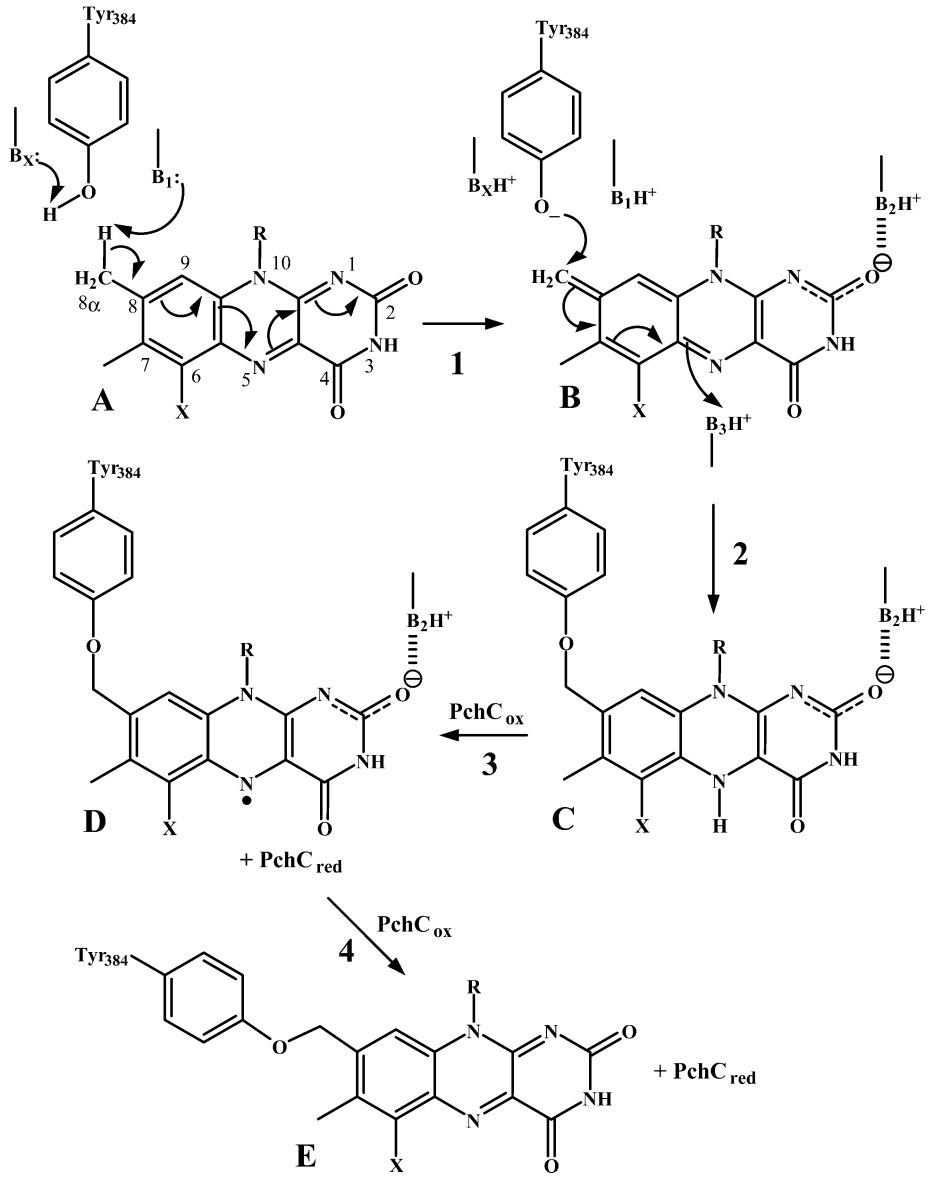

FIGURE 1: Mechanism of covalent flavinylation of PchF. B_1, B_2, B_3, and B_x are hypothetical bases required for the flavinylation process. From the crystal structure of PCMH, B_2 has been identified as Arg474 (*1*). Because of its proximity, B_3 could be Glu380. Due to lack of proximity, it is not possible to definitively identify B_1 or B_x. It is possible that the phenolate form of Tyr384 acts as B_1, and B_x may be Asp440, which is hydrogen bonded to a water molecule (2.49 Å) that is also hydrogen bonded to the phenolate group of Tyr384 (3.09 Å). R represents the ribityl diphosphoadenosine moiety, and X can be H, NH_2, or Br. Structure B is the putative iminoquinone methide-like intermediate that is believed to be the electrophilic species that is attacked by the tyrosinate nucleophile at the 8α-carbon of the isoalloxazine ring. The covalent flavinylation process results in 2-electron-reduced 8α-tyrosyl-*O*-FAD (structure C). The electrons are shuttled rapidly, one at a time to PchC. The reduced heme is oxidized subsequently by an external electron acceptor.

and $PchF^{NC}$ form a weak complex to produce PCMH-$\{FAD\}^{NC}$. Ensuing conformational changes lead to the covalent tethering of FAD to yield mature PCMH$\{FAD\}^{C}$. The fully reduced FAD formed in this process shuttles its electrons sequentially and rapidly from the enzyme, via the heme of PchC, to yield oxidized PCMH$\{FAD\}^{C}$ (Figure 1). For FAD, $E_{m,7}$ rises from −16 mV for $PchF^{NC}$ to +87 mV in PCMH$\{FAD\}^{C}$. For the heme, the 1-electron potential rises from +157 mV for free PchC to +234 mV in the flavocytochrome (*6*).

$PchF\{FAD\}^{C}$ has an $E_{m,7}(FAD) = +62$ mV (*6*). The large 78 mV increase in $E_{m,7}$(FAD) for $PchF^{C}$ relative to that for $PchF^{NC}$ indicates that structural alterations in the former significantly stabilize reduced, bound FAD relative to its oxidized form. While a great deal of the change in $E_{m,7}$(FAD) is due to the covalent tethering, other (structural, environmental, etc.) factors contribute to the potential change from +62 to + 87 mV when $PchF^{C}$ binds to PchC.

For PchF[Y384F]$\{FAD\}^{NC}$ and PCMH[Y384F]$\{FAD\}^{NC}$, Phe has replaced Tyr384, the residue that is covalently linked to FAD in normal PCMH. Hence, FAD cannot bind covalently to the mutant proteins. The $E_{m,7}$(FAD) values for PchF[Y384F]$\{FAD\}^{NC}$ and PCMH[Y384F]$\{FAD\}^{NC}$ are +2 and +47 mV, respectively (*6*). Assuming that a similar change occurs for the $PchF\{FAD\}^{NC}$ to PCMH$\{FAD\}^{NC}$ transition, $E_{m,7}$(FAD) is estimated to be about +30 mV for the latter protein. Thus, it is predicted that covalent binding of FAD in PCMH$\{FAD\}^{NC}$ results in an increase in $E_{m,7}$(FAD) of about 57 mV (87 mV − 30 mV). The change in $E_{m,7}$(FAD) for $PchF\{FAD\}^{NC}$ from −16 to +57 mV on binding to PchC increases the electrophilicity of the flavin's isoalloxazine ring for PCMH$\{FAD\}^{NC}$. We proffer that this

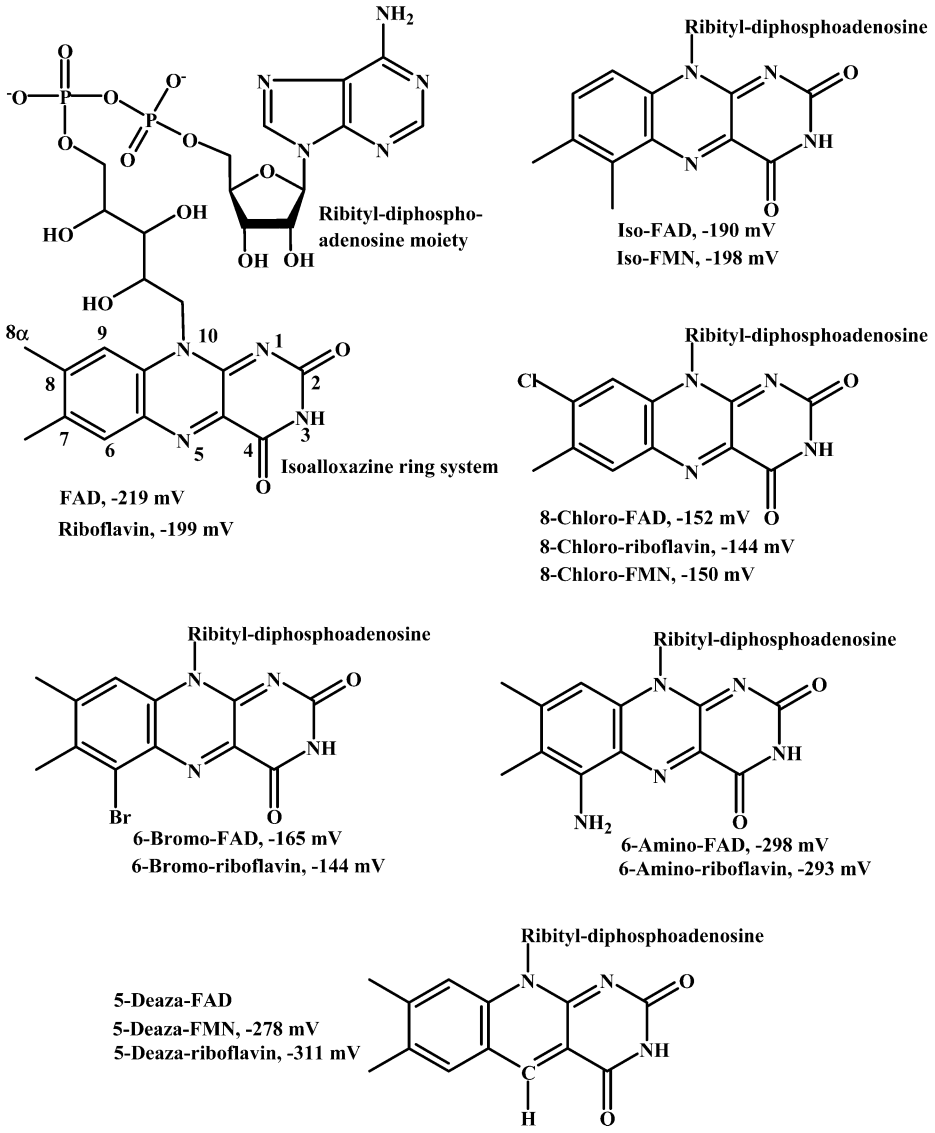

FIGURE 2: Structures and values of the 2-electron redox potential, $E_{m,7}$, for the flavins used in the current study. The potentials are from the following references: Rbf, FAD, 8-Cl-Rbf, and 8-Cl-FMN (*8*); iso-FMN and 5-deaza-FMN (*9*); 5-deaza-Rbf (*8*, *10*); 6-NH_2-Rbf and 6-Br-Rbf (*8*, *11*); iso-FAD, 8-Cl-FAD, 6-NH_2-FAD, and 6-Br-FAD (this study).

increases also the acidity of its 8α-methyl hydrogens to facilitate formation of a flavin iminoquinone methide-type species, a putative intermediate for covalent flavinylation (structure B, Figure 1) (*4*).

The 1-electron heme potential for PCMH[Y384F]{FAD}^{NC} is +187 mV, 50 mV lower (*6*) than the potential for PCMH{FAD}^{C}. This implies that covalent tethering of FAD in PCMH{FAD}^{NC} produces conformational and/or electrostatic changes in PchC that stabilize the reduced heme relative to its oxidized form. In addition, the affinity of PchF[Y384F]{FAD}^{NC} for PchC (K_D = 7.4 μM) is 3 orders of magnitude less than that of PchF{FAD}^{C} for PchC (K_D = 7.4 nM) (*7*). Thus, covalent flavinylation results in favorable potential changes for both FAD and heme and favorable subunit interactions in PCMH. The information presented in the preceding paragraphs is summarized in Figure S1 (Supporting Information).

It was discovered also that the covalent FAD bond in free PchF or PCMH is very stable; on reduction, the covalent bond remains intact. In sharp contrast, free in solution, reduced 8α-*O*-tyrosylriboflavin very rapidly expels tyrosine to yield oxidized riboflavin (Rbf) (*2*).

These interesting features of PchF make it well suited for studies of the relationships between structure and redox properties and catalysis. For example, we can compare the chemical, physical, redox, etc. characteristics of three forms of PchF, i.e., PchF{FAD}^{NC}, PchF{FAD}^{C}, and PCMH-{FAD}^{C}. We can also easily produce apo-PchF and reconstitute it with FAD analogues that bind noncovalently (*5*), some of which can be induced to bind covalently. Interestingly, for PchF harboring 6-amino-FAD (6-NH_2-FAD) (Figure 2), because the covalent flavinylation process is extremely slow (vide infra), we can study the properties of four forms of this flavoprotein: PchF{6-NH_2-FAD}^{NC}, PchF{6-NH_2-FAD}^{C}, PCMH{6-NH_2-FAD}^{NC}, and PCMH-{6-NH_2-FAD}^{C}. Further, site-specifically altered forms of PchF can be used. Thus, we are able to extend easily the repertoire of proteins for investigation.

The flavins employed in the current work have structural alterations at sites that dramatically alter the physical, chemical, binding, and/or redox properties of the isoalloxazine ring (Figure 2) (*12*). After each Rbf analogue was converted to the corresponding FAD form (*13*), the spectral properties of each of these were studied. Further, the spectral

changes of flavin-reconstituted forms of PchF and PCMH were recorded during titrations with (nonreducing) substrate analogues and reductive titrations with dithionite or substrates. For each protein, the 2-electron midpoint redox potential, $E_{m,7}$, of the flavin was determined also (*14*). Herein, we present the results and conclusions derived from our investigations.

EXPERIMENTAL PROCEDURES

Materials. 6-Amino-Rbf (6-NH_2-Rbf) was synthesized as described elsewhere (*11*). *p*-Cresol, 4-hydroxybenzyl alcohol, 4-hydroxybenzaldehyde, and 4-Br-phenol were purified as before (*3*). Other chemicals used in the studies and their sources are as follows: 8-nor-8-chloro-Rbf (8-Cl-Rbf), 6-bromo-Rbf (6-Br-Rbf), and 5-deaza-5-carba-Rbf (5-deaza-Rbf), gifts from Peter Hemmerich (deceased) and Sandro Ghisla (University of Konstanz, Germany); disodium 2,6-dichlorophenolindophenol (DCIP), General Biochemicals, Inc.; sodium dithionite, Kodak Chemical Co.; iso-Rbf (8-demethyl-6-methyl-Rbf), Merck; glucose oxidase, Miles Laboratories; toluylene blue, ICN Pharmaceuticals, Inc.; thionin, Janssen Chimica; anthroquinone-2,6-disulfonate disodium salt and 5,5′,7,7′-indigotetrasulfonate tetrapotassium salt, Aldrich Chemical Co.; gallocyanine, 5,5′-indigodisulfonate disodium salt (Indigo Carmine), methylene blue, Nile Blue, 5,5′,7-indigotrisulfonate tripotassium salt, phenosafranine, safranine O, and toluidine blue O, Sigma Chemical Co.; ammonium acetate, International Biotechnologies, Inc.; other reagents, Sigma Chemical Co. or Aldrich Chemical Co.

Purification of PchF and PchF[Y384F]. The growth of transformed *E. coli* strains and the protein purification are described in detail elsewhere (*3*, *15*). The pure proteins were devoid of type *c* cytochromes and bound FAD. Centricon-30 centrifuge concentrators (Amicon, Inc.) were used for buffer exchanges.

Isoelectric Focusing (IEF). PCMH containing either covalently bound FAD, 6-NH_2-FAD, or 6-Br-FAD was processed by IEF, which separated the $PchF^C$ forms from PchC and apo-PchF (*5*). Pharmalyte 4-6.5 ampholytes were used for the IEF, which was done in a thin layer of prehydrated Sephadex G-200 Superfine (Amersham Pharmacia Biotech).

FAD Analogues. FAD derivatives were obtained from the corresponding Rbf analogues (~200 μM) by room temperature incubation in 25 mM potassium phosphate buffer, pH 7.6, with 200 nM pure *Corynebacterium ammoniagenes* FAD synthetase, 3−5 mM ATP, and 10 mM $MgCl_2$ (*13*, *16*). After a reaction had reached an acceptable level as determined by HPLC analysis, each FAD analogue was purified using a 150 × 4.6 mm Spherex 3-μm octadecyl-silica gel column (Phenomenex, Inc.) that was preequilibrated with aqueous 10 mM ammonium acetate. The sample was eluted with a 20 min gradient from 100% 10 mM ammonium acetate to 50% acetonitrile, at room temperature, with a 1 mL/min flow rate. Each FAD analogue, and its FMN and Rbf counterparts, eluted at approximately ~4, ~4.8, and ~6 min, respectively. Each collected fraction was lyophilized.

The authenticity of each FAD analogue was confirmed by a reverse reaction catalyzed by FAD synthetase; in the presence of $MgCl_2$ and pyrophosphate, FAD is converted to FMN and ATP (*13*). Further proof was obtained by treating a portion of the sample with nucleotide pyrophosphatase, which converted FAD to FMN and AMP. The disappearance of FAD and appearance of FMN were followed by HPLC (vide supra). Final proof was obtained by demonstrating that all FAD analogues bound quickly and avidly to apo-PchF. Neither FMN nor Rbf binds to this protein (*4*). Although all of the Rbf analogues tested were substrates for FAD synthethase, the conversion rates varied: ~100% of 5-deaza-Rbf and 6-NH_2-Rbf were converted to the FAD forms after 1 hour, whereas ~50% of iso-Rbf and 8-Cl-Rbf and ~10% of 6-Br-Rbf were converted to the FAD counterparts after several days.

Kinetic Assays. Kinetic experiments, titrations, and redox potential measurements were typically done in 25 mM KH_2PO_4/KOH buffer, pH 7.0 at 25 °C. Steady-state kinetic spectrophotometric assays were carried out by using *p*-cresol as the reducing substrate and phenazine ethosulfate (PES) as the reoxidizing substrate (*17*). The reduced PES that formed was monitored at 600 nm due to its reduction of 2,6-dichlorophenolindophenol.

Covalent flavinylation reactions were carried out by mixing various forms of $PchF^{NC}$ with PchC as reported elsewhere (*4*). The reactions were monitored by following the heme reduction spectrophotometrically (Figure 1). To avoid interference with flavin and subsequent heme reduction that occur during covalent flavinylation (Figure 1), these reactions were done in the dark to prevent flavin-dependent photoreduction of the prosthetic groups.

Spectroscopy and Titrations. UV−visible spectra were obtained with a Hewlett-Packard 8453A diode array spectrophotometer. Sets of spectra for each titration were analyzed by SPECFIT (factor analysis software from Spectrum Software Associates, Chapel Hill, NC). Anaerobic dithionite- and substrate-reductive titrations and $E_{m,7}$ measurement experiments were carried out under Ar in anaerobic quartz cuvettes (*18*). Because of *p*-cresol's volatility, its solutions were made anaerobic by the presence of glucose, glucose oxidases, and catalase (*17*). Other solutions were rendered anaerobic with several vacuum/O_2-free Ar-flushing cycles. Unless noted otherwise, $E_{m,7}$ values were determined by using the xanthine/xanthine oxidase method of Massey, which required the presence of methyl viologen and a reference dye with an appropriate redox potential (*14*). The dithionite titrations provided the extinction coefficients for the flavins bound to the various proteins. The concentrations of dithionite solutions were determined by titrating anaerobic solutions of FAD (ϵ_{450} = 11.7 mM^{-1} cm^{-1}).

RESULTS

Spectral Properties of Variant Forms of PchF and PCMH. Because of the large number of proteins studied, we have omitted figures and the details for some of the spectral titrations and potential measurements. Within this report, we have included representative or interesting figures for a few of the cases. Some figures can be found in the Supporting Information. The $E_{m,7}$ values and the data for the 4-Br-phenol CT complexes are presented in Table 1. The data for some of the derivatives discussed herein can be found elsewhere (*3*, *6*, *15*).

Table 1: Redox Potentials for Various Forms of PCMH and PchF and Data for 4-Br-phenol Binding to These Proteins

protein	k_{cat} (s^{-1})	$E_{m,7}$ (mV) [slope][a]	reference dye, $E_{m,7}$ (mV)	K_D[b] (μM)	λ_{max}[b] (nm)
PchF{FAD}^{NC} [c]	0.75	−15.6 [0.93], −13.3 [1.00]	gallocyanine, 21	58	620
PchF{FAD}^{C} [c]	0.080	59.5 [1.07], 60 [0.95]	thionin, 60	18	655
		60 [1.11], 65.5 [0.98]	toluidine blue O, 34		
		66 [1.06]	toluylene blue, 115		
PCMH{FAD}^{C} [c]	121			ND[e]	833
FAD[d]		87 [0.99], 81 [1.09]	toluylene blue, 115		
heme		249 [1.97]	DCIP, 218		
PchC[c]		157 [1.98]	toluylene blue, 115	NA[f]	NA
		157 [2.05]	DCIP, 218		
PchF[Y384F]{FAD}^{NC} [c]	0.22	2 [0.94], 1.2 [0.92]	gallocyanine, 21	6	630
		3[g]	juglone, 3		
PCMH[Y384F]{FAD}^{NC} [c]	3.8			ND	698
FAD[d]		49 [1.06], 46 [1.05]	toluidine blue O, 34		
		45.5 [1.07]	thionin, 60		
heme		186 [2.02]	DCIP, 218		
PchF{iso-FAD}^{NC}	0.0080	−104 [1.00]	5,5′,7-indigotrisulfonate, −81	6 ± 1.5	603
		−110 [1.06]	Nile Blue, −116		
PCMH{iso-FAD}^{NC}	0.55			ND	647
iso-FAD[d]		33 [0.99]	toluidine blue O, 34		
		30 [1.00]	gallocyanine, 21		
heme		206 [1.99]	DCIP, 218		
PchF{5-deaza-FAD}^{NC}	0.0030	ND[i]		ND	536
PCMH{5-deaza-FAD}^{NC} [h]	0.42			ND	621
5-deaza-FAD[d]		18 [1.04]	gallocyanine, 21		
		15 [1.07]	methylene blue, 11		
PchF[Y384F]{5-deaza-FAD}^{NC}	0.00096	−300 [1.07]	safranine O, −289	ND	524
PCMH[Y384F]{5-deaza-FAD}^{NC}	0.44	ND[i]		ND	593
PchF{6-NH_2-FAD}^{NC}	0.10	−276 [0.94]	phenosafranine, −252	ND	546
PchF{6-NH_2-FAD}^{C}	0.013	−252 [1.07]	phenosafranine, −252	21 ± 10	583
PCMH{6-NH_2-FAD}^{NC} [h]	0.085			ND	615
6-NH_2-FAD[d]		−187 [1.16]	anthraquinone-2,6-disulfonate, −184		
PCMH{6-NH_2-FAD}^{C} [h]	0.21			ND	627
6-NH_2-FAD[d]		−174 [1.16]	anthraquinone-2,6-disulfonate, −184		
PchF{6-Br-FAD}^{NC}	ND[j]	−128 [1.03], −136 [0.93]	5,5′-indigodisulfonate, −125	ND	ND
PchF{6-Br-FAD}^{C}	0.070	−48 [1.01], −59 [1.04]	5,5′,7,7′-indigotetrasulfonate, −46	ND	641
PCMH{6-Br-FAD}^{C} [h]	1.3			ND	665
6-Br-FAD[c]		60 [1.08]	gallocyanine, 21		
		65 [1.07]	thionin, 60		
PchF{8-Cl-FAD}^{NC}	0.19	16 [1.02]	toluidine blue O, 34	ND	649
PCMH{8-Cl-FAD}^{NC} [h]	18.3			ND	781
8-Cl-FAD[d]		90 [1.03]	thionin, 60		
PchF[Y384F]{8-Cl-FAD}^{NC}	0.22	59 [1.04]	thionin, 60	ND	653
		63 [1.03]	toluidine blue O, 34		
PCMH[Y384F]{8-Cl-FAD}^{NC} [h]	3.80			ND	798
8-Cl-FAD[d]		104 [1.02]	toluylene blue, 115		

[a] Slopes for the $RT/2\mathcal{F} \times \ln(dye_{ox}/dye_{red})$ vs $RT/2\mathcal{F} \times \ln(P_{ox}/P_{red})$ plots, where P represents the protein and R, T, and $\mathcal{F}$ are the gas constant, the temperature, and Faraday's constant, respectively. Slopes of ~1 indicate that these are the 2-electron potentials for the flavin. A slope of ~2 is expected for the 1-electron reduction of the heme. [b] For some of the proteins, the values for K_D and λ_{max} of the flavin's CT peaks were determined from 4-Br-phenol spectrophotometric titrations. For the remaining proteins, the λ_{max} values were determined from spectra after addition of a saturating concentration of 4-Br-phenol. [c] Data from refs *6* and *15*. [d] Because of its high potential, the heme groups of the various PCMH forms were completely reduced when the potential of the flavins was measured. [e] Not determined. [f] Not applicable. [g] The potential was determined by factor analysis, not graphically; thus a slope is not available (*6*). [h] The heme potential was not determined. [i] Not determined. See text. [j] Rate of oxidation was very low.

All of the forms of PCMH and PchF studied had *p*-cresol oxidation activity. However, a detailed analysis and discussion of the catalytic efficiency are presented elsewhere (*19*).

PchF{iso-FAD}^{NC}. Figure 3 shows the spectral changes for the dithionite titrations of free iso-FAD and PchF{iso-FAD}^{NC}. Free iso-FAD has absorbance maxima at 456 nm (ϵ = 7.70 mM^{-1} cm^{-1}) and 386 nm (10.9 mM^{-1} cm^{-1}), which are similar to those reported earlier (*20*). When bound to PchF, the maxima shifted to 444 nm (ϵ = 7.20 mM^{-1} cm^{-1}) and 388 nm (ϵ = 12.8 mM^{-1} cm^{-1}), respectively. For the PchF{iso-FAD}^{NC} titration, the first addition of dithionite caused a slight decrease in absorbance at 382 nm, which was followed by a slight increase (Figure 3B). On further additions, the 382 nm absorbance decreased progressively. These changes and the sharp absorbance peak at 382 nm indicate the formation and subsequent disappearance of an iso-FAD radical as more dithionite was added (*17*, *21*). Corresponding spectral changes were not seen for protein-free iso-FAD during its dithionite titration (Figure 3A), indicating that a stable flavin radical did not form.

The 4-hydroxybenzyl alcohol reduction of PchF{iso-FAD}^{NC} progressed very slowly, particularly in the latter stage of the titration. Initially, as the flavin absorbance bleached, an absorbance peak appeared at 343 nm. This was due to a complex between the remaining oxidized PchF(iso-FAD)^{NC} and 4-hydroxybenzaldehyde, the product of alcohol oxidation by the enzyme. A flavin radical was not detected during the titration.

The results of the factor analysis of spectral data for the aerobic titration of PchF{iso-FAD}^{NC} with 4-hydroxybenz-

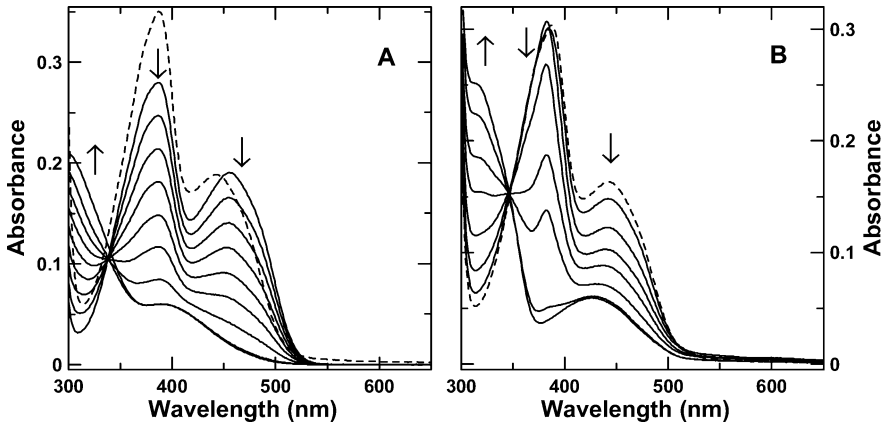

FIGURE 3: Anaerobic dithionite titrations of iso-FAD and PchF{iso-FAD}^{NC}. Frame A displays the spectra recorded during the dithionite titration of 24 μM iso-FAD in 25 mM KH_2PO_4/KOH, pH 7.0 at 25 °C. The dashed line, which depicts the spectrum for the fully oxidized form of PchF{iso-FAD}^{NC}, is included for comparison. The cumulative concentrations of added dithionite were 0, 3.53, 7.05, 10.6, 14.1, 17.6, 21.1, 24.6, and 28.0 μM. The arrows indicated the changes that occurred as progressively more dithionite was added. Frame B displays the spectra recorded during the dithionite titration of 21 μM PchF{iso-FAD}^{NC} in 25 mM KH_2PO_4/KOH, pH 7.0 at 25 °C. The dashed line represents the spectrum of the fully oxidized enzyme. The cumulative concentrations of added dithionite were 0, 3.53, 7.05, 10.6, 14.1, 17.6, 21.1, and 24.6 μM. The arrows indicated the changes that occurred as progressively more dithionite was added. Note that the absorbance at 382 nm decreases slightly initially and then increases slightly. The relatively sharp peak is believed to be due to the presence of a flavin radical, which appeared in the initial phase of the titration and then disappeared as more reductant was added.

aldehyde are presented in Figure S2A (Supporting Information). The increase in absorbance at wavelengths >500 nm and decreases from 370 to 500 nm indicated the formation of an iso-FAD−aldehyde charge-transfer (CT) complex (*3*). A $K_D = 0.20 \pm 0.05$ μM for the complex confirmed the very tight binding of the aldehyde to oxidized PchF{iso-FAD}^{NC} (vide supra). The very large absorbance at 343 nm (Figure S2A) indicates that the aldehyde is bound as an anionic quinone methide-type species (*3*); compare this absorbance to that of enzyme-free aldehyde (Figure S2A).

It was established previously that the $E_{m,7}$ for the 4-hydroxybenzyl alcohol/4-hydroxybenzaldehyde couple is considerably more negative than that for the *p*-cresol/4-hydroxybenzyl alcohol couple (*3*). Accordingly, while reduction by the alcohol was slow, *p*-cresol did not reduce PchF{iso-FAD}^{NC} to an appreciable extent. Figure S2B (Supporting Information) shows the results of a rapid aerobic, nonreductive titration of PchF{iso-FAD}^{NC} by *p*-cresol. The formation of a CT transition band is evident from the increase in absorbance from 500 to 800 nm. An analysis of the absorbance changes for the titration provided a $K_D = 3.2 \pm 1.4$ μM.

Figure S2C (Supporting Information) shows the alteration to the PchF{iso-FAD}^{NC} spectrum resulting from the CT interaction with 4-Br-phenol. The position of the maximum of the CT band was estimated to be 620 nm, and the complex has a $K_D = 6 \pm 1.5$ μM.

PCMH{iso-FAD}^{NC}. Since iso-FAD lacks an 8-methyl group on its isoalloxazine ring (Figure 2), it is unable to bind covalently when PchF{iso-FAD}^{NC} is mixed with PchC (*4*). The addition of a equimolar amount of PchC to PchF{iso-FAD}^{NC} raised the $E_{m,7}$(iso-FAD) (Table 1) enough so that *p*-cresol reduction of the resulting PCMH{iso-FAD}^{NC} proceeded at a convenient rate. However, the steady-state turnover rates were significantly lower for PCMH{iso-FAD}^{NC} and PchF{iso-FAD}^{NC} when compared to PCMH-{FAD}^{C} and PchF{FAD}^{NC} or PchF{FAD}^{C}.

As with PCMH, for the anaerobic *p*-cresol titration of PCMH{iso-FAD}^{NC}, the first electron equivalent contributed to the complete, 1-electron reduction of the heme. The next two electron equivalents resulted in the full, 2-electron reduction of iso-FAD. The stepwise reduction indicates that reduced flavin to oxidized heme electron transfer is not prohibited by the absence of a covalent bond between the flavin and protein (*1*). Since *p*-cresol donates 2 electrons to the bound iso-FAD and 1 electron must be transferred rapidly from PchF{iso-FAD}^{NC} to the heme of PchC bound to this PchF subunit, then either the second electron stays with iso-FAD (i.e., a flavin radical would accumulate) or, somehow (as is the case), this electron is transferred efficiently from the flavin radical to a second oxidized heme group. The $E_{m,7}$(iso-FAD) = +30−33 mV for PCMH{iso-FAD}^{NC} (Figure S3, Supporting Information) (Table 1). Hence, $E_{m,7}$(iso-FAD) rises by ~130 mV when PchF{iso-FAD}^{NC} binds to PchC. The potential of the heme of PchC increases also when this interaction occurs (Table 1).

PchF{5-deaza-FAD}^{NC}. 5-Deaza-FAD bound stoichiometrically to apo-PchF, as determined by fluorescence quenching. The absorbance maximum at 400 nm for free 5-deaza-FAD shifted to 394 nm. Since the anaerobic reduction of PchF{5-deaza-FAD}^{NC} with dithionite was so slow, it was not possible to estimate the extinction coefficient for this enzyme; it was assumed to be equal to that of free 5-deaza-Rbf (12.6 mM^{-1} cm^{-1}) (*10*). An excess of dithionite was needed to fully reduce the flavin. On admission of air, the reduced flavin did not reoxidize, even after a prolonged incubation. The complete O_2 oxidation of reduced FAD or other FAD analogues bound to PchF occurred within a few minutes after being exposed to air. These observations imply that the reduction of O_2 by the reduced flavins bound to PchF involves 1-electron steps (*22*). Since the formation of the 5-deaza-FAD radical is thermodynamically unstable, then it is expected that the reduction of O_2 by reduced 5-deaza-FAD would be extremely slow. For free 5-deaza-Rbf, $E_1 = -650$ mV, whereas the 2-electron $E_{m,7}$ is −311 mV.

We could not identify any agents that reoxidized reduced PchF{5-deaza-FAD}^{NC}, except for PES, which allowed measurements of its catalytic activity in steady-state kinetic

assays. Thus, an equilibrium redox titration with reference dyes was impossible. This disallowed the measurement of the $E_{m,7}$ value for the bound 5-deaza-FAD.

PchF{5-deaza-FAD}^{NC} was not reduced by *p*-cresol. An aerobic titration with *p*-cresol revealed the formation of a CT complex ($K_D = 2.95 \pm 1.40$ μM). For the anaerobic 4-hydroxybenzyl alcohol titration of PchF{5-deaza-FAD}^{NC}, the reduction of the bound flavin occurred slowly. The titration proceeded with the intermediate formation of a complex between the bound oxidized 5-deaza-FAD and the anionic quinone methide form of the alcohol's oxidation product, 4-hydroxybenzaldehyde (see Figure 8); a large absorbance peak appeared at 342 nm due to the complex, which disappeared subsequently as the remaining oxidized flavin was very slowly reduced by the alcohol.

A factor analysis of the spectra recorded during a 4-hydroxybenzaldehyde titration of PchF{5-deaza-FAD}^{NC} indicated the formation of a tight complex, with $K_D = 0.53 \pm 0.3$ μM. The spectrum of the complex, with a weak CT band at 450−500 nm, also displayed the large absorbance peak at 343 nm similar to that seen for the aldehyde complexes for PchF{iso-FAD}, PchF{FAD}^{C}, PchF[Y384F]-{FAD}^{NC}, and other forms of PchF (*3*, *15*). This indicated that the aldehyde is bound as an anionic quinone methide-type species (*3*).

PchF[Y384F]{5-deaza-FAD}^{NC}. The PchF[Y384F] mutant (*6*) also bound 5-deaza-FAD tightly. The binding produced a shift from 400 nm for the free flavin to 393 nm in the protein, and the spectrum of the latter has some resolution in its vibrational modes in its long-wavelength (393 nm) absorbance peak. When the protein was titrated with 4-hydroxybenzyl alcohol, initially, a 342 nm peak appeared, which was a result of the product, 4-hydroxybenzaldehyde, binding to oxidized PchF[Y384F]{5-deaza-FAD}^{NC} (vide supra). This peak shifted to 332 nm when the aldehyde dissociated as flavin reduction progressed.

The $E_{m,7}$(5-deaza-FAD) = −300 mV for this protein. Only the flavin that became reduced in the initial stages of the titration was in equilibrium with the dye; the ln(protein$_{ox}$/protein$_{red}$) vs ln(dye$_{ox}$/dye$_{red}$) plot for this part of the experiment provided a slope of ∼1. For computational purposes, the complete reduction of flavoprotein was achieved by adding dithionite. The value of $E_{m,7}$ is similar to that of free 5-deaza-FMN (−278 mV) (*9*). It was not possible to determine $E_{m,7}$ for the flavin for PCMH[Y384F]{5-deazaFAD}^{NC}.

PCMH{5-deazaFAD}^{NC}. Although 5-deaza-FAD has a methyl group at the 8-position of the flavin ring, covalent flavinylation did not occur, as judged by heme reduction, when PchF{5-deaza-FAD}^{NC} was mixed anaerobically in the dark with PchC.

A dithionite titration of PCMH{5-deaza-FAD}^{NC} showed a fast 1-electron reduction of the heme group followed by an extremely slow reduction of the bound flavin. PCMH-{5-deaza-FAD}^{NC} was also titrated anaerobically with *p*-cresol. Full reduction of the cytochrome subsystem (6 μM) was achieved when the total concentration of added *p*-cresol reached 1.5 μM, as expected for a stoichiometric process; this substrate supplies 4 electron equivalents when it is oxidized completely to the final product, 4-hydroxybenzaldehyde. Complete reduction of the bound flavin required a further 0.5 molar equiv of *p*-cresol. Hence, this titration proceeded in the same manner as that for PCMH{FAD}^{C} (*23*).

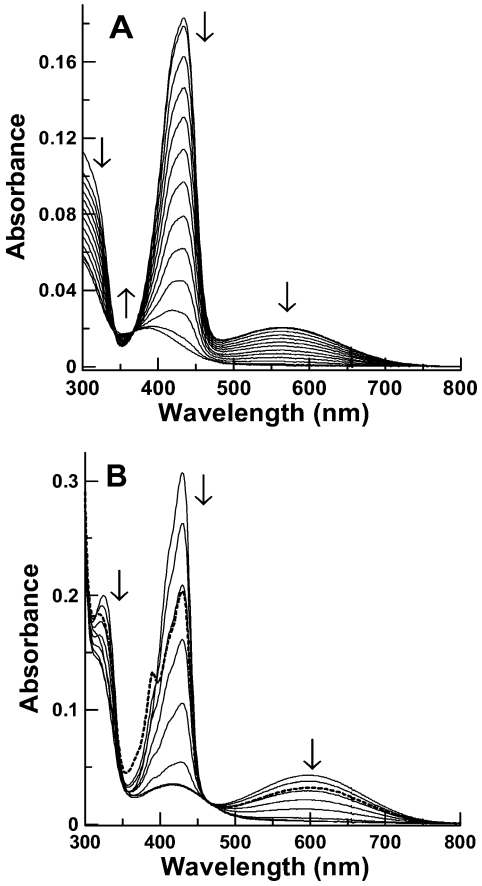

FIGURE 4: Anaerobic dithionite titrations of 6-NH$_2$-FAD and PchF{6-NH$_2$-FAD}^{NC}. Frame A shows the dithionite titration of 11.3 μM 6-NH$_2$-FAD in 25 mM KH$_2$PO$_4$/KOH, pH 7.0 at 25 °C. The cumulative concentrations of added dithionite were 0, 1.02, 2.04, 3.06, 4.08, 5.09, 6.10, 7.11, 8.11, 9.12, 10.1, 11.1, and 12.1 μM. The arrows indicated the changes that occurred as progressively more dithionite was added. Frame B shows the dithionite titration of 13 μM PchF{6-NH$_2$-FAD}^{NC} in 25 mM KH$_2$PO$_4$/KOH, pH 7.0 at 25 °C. The cumulative concentrations of added dithionite were 2.19, 4.38, 6.56, 8.73, 10.9, 13.0, 15.2, and 17.3 μM. The arrows indicated the changes that occurred as progressively more dithionite was added. The thick dashed line represents the spectrum recorded immediately after the second (4.38 μM) addition of dithionite. The small sharp peak at ∼380 nm for the dashed line spectrum is believed to arise from the presence of a small amount of a flavin radical. This spectral feature disappeared within 15 min. This feature was seen also for the spectra obtained after the other additions of dithionite. However, all of the other (end point) spectra were obtained about 15 min after the addition of dithionite.

The $E_{m,7}$(5-deaza-FAD) value for PCMH{5-deaza-FAD}^{NC} is provided in Table 1. During the potential measurement experiment, the reduction of the flavin was slow, so excess sodium dithionite was added near the end in order to achieve full reduction and an accurate end point.

PchF{6-NH$_2$-FAD}^{NC}. The properties of 6-NH$_2$-Rbf are described elsewhere (*11*). Its spectrum shows a narrow band in the 390−430 nm region and a broad pH-sensitive band centered at 560 nm. Figure 4A shows the solution spectrum of 6-NH$_2$-FAD. A dithionite titration of the free flavin provided $\epsilon_{436} = 16.1$ mM^{-1} cm^{-1} (Figure 4A), which is somewhat lower than the $\epsilon_{428} \approx 19$ mM^{-1} cm^{-1} for 6-NH$_2$-Rbf. The lower absorbance and red shift are characteristic

for a Rbf to FAD transition. The broad peak for 6-NH_2-FAD centered at 566 nm corresponds to the broad peak for 6-NH_2-Rbf that has a maximum at 560 nm. The absence of a peak between 300 and 400 nm indicates that the amino group of 6-NH_2-FAD is unprotonated and that it exists as the iminoquinonoid form (see structure B, Figure 7), which exists between pH 0.9 and pH 10.3 (*11*).

6-NH_2-FAD bound tightly and stoichiometrically to apo-PchF. The spectrum of PchF{6-NH_2-FAD}^{NC} (Figure 4B) showed that the 560 nm band has shifted to 602 nm, relative to that for the free flavin, and a new, narrow peak appeared at 327 nm. The basic spectral features indicate that 6-NH_2-FAD is bound to PchF with the isoalloxazine ring in the neutral iminoquinonoid form.

The dithionite titration of PchF{6-NH_2-FAD}^{NC} revealed the formation of an unstable (presumably anionic) radical, detectable by perturbations in the 385 nm region of the spectrum (Figure 4B). This feature disappeared within 15 min due to disproportionation of the radical. From the titration data, $\epsilon_{432} = 22.6$ mM^{-1} cm^{-1} was determined.

PchF{6-NH_2-FAD}^{NC} was not reduced by *p*-cresol or 4-hydroxybenzyl alcohol at reasonable rates, and a CT complex between *p*-cresol and PchF{6-NH_2-FAD}^{NC} was not detected. The value of $E_{m,7}$ for free 6-NH_2-FAD was found to be -298 mV, which is similar to that for 6-NH_2-Rbf ($E_{m,7} = -293$ mV) (*11*). For PchF{6-NH_2-FAD}^{NC}, $E_{m,7} = -276$ mV (Table 1). This very low redox potential explains why the enzyme was not reduced easily by substrates.

PchF{6-NH_2-FAD}^{C}. Because of its low potential, it was assumed that, like PchF{5-deaza-FAD}^{NC}, the flavin would not bind covalently to PchF{6-NH_2-FAD}^{NC} when exposed to PchC. However, after 2 days at room temperature, a small amount of PCMH{6-NH_2-FAD}^{C} formed. Enough PchF{6-NH_2-FAD}^{C} was isolated by IEF for us to determine $E_{m,7}$(6-NH_2-FAD) (Table 1). Treatment of a solution of this protein with 5% (w/v) trichloroacetic acid, followed by centrifugation, gave a green pellet with no free flavin in solution. This indicated that 6-NH_2-FAD was covalently bound stably to the protein (*24*).

Like that for PchF{6-NH_2-FAD}^{NC} (Figure 4B), the spectrum for PchF{6-NH_2-FAD}^{C} displayed a narrow, intense band at ~420 nm ($\epsilon = 20000$ M^{-1} cm^{-1}) and a less intense, broad peak centered at ~600 nm ($\epsilon = 2200$ M^{-1} cm^{-1}) (Figure S4, Supporting Information). When PchF{6-NH_2-FAD}^{C} was titrated with dithionite, a very slow reduction of the flavin occurred after each addition of the reductant. The titration proceeded with the intermediate formation of a (presumably anionic) radical (Figure S4). The stable end point spectra for each addition of the reductant indicated that the radical was thermodynamically stable (*6*). The maximum amount of radical formed was 47% of the total bound flavin. From the equation $([Fl_{rad}]/[Fl]_t)_{max} = 0.47 = K^{1/2}/(2 + K^{1/2})$ (*25*), the radical formation constant $K = 3.15$. $\Delta E = 29$ mV is determined from the relationship $\Delta E = E_1 - E_2 = (RT/\mathcal{F}) \ln(K)$, where E_1 is the 1-electron potential for the reduction of oxidize bound 6-NH_2-FAD and E_2 is the 1-electron potential for the radical reduction step (*6*, *25*). Since $(E_1 + E_2)/2 = E_{m,7} = -252$ mV, then $E_1 = E_{m,7} + \Delta E/2 = -252 + 14.5 = -238$ mV, and $E_2 = E_{m,7} - \Delta E/2 = -252 - 14.5 = -267$ mV.

PCMH{6-NH_2-FAD}^{NC}. It was found that the flavin very slowly became covalently bound in an equimolar mixture of PchF{6-NH_2-FAD}^{NC} and PchC. This indicates that the bound 6-NH_2-FAD is a poor electrophile, which is corroborated by its low redox potential. The very slow covalent flavinylation process allowed us to study PCMH{6-NH_2-FAD}^{NC}.

Both *p*-cresol and 4-hydroxybenzyl alcohol reduced the heme in PCMH{6-NH_2-FAD}^{NC}. These titrations proceeded in the same manner as those for normal PCMH (*23*). When the heme is fully reduced, $E_{m,7}$(6-NH_2-FAD) $= -187$ mV.

PCMH{6-NH_2-FAD}^{C}. $E_{m,7}$(6-NH_2-FAD) $= -174$ mV for PCMH{6-NH_2-FAD}^{C}, 13 mV more positive than the $E_{m,7}$ value for PCMH{6-NH_2-FAD}^{NC}. PCMH{6-NH_2-FAD}^{C} had about twice the activity of PCMH{6-NH_2-FAD}^{NC}. The λ_{max} of the 4-Br-phenol CT band was shifted to 627 nm, as compared to 615 nm for PCMH{6-NH_2-FAD}^{NC}.

PchF{6-Br-FAD}^{NC} and PchF{6-Br-FAD}^{C}. After heme reduction ceased for a mixture of PchF{6-Br-FAD}^{NC} and PchC, the resulting flavocytochrome was subjected to IEF, which yielded pure PchF{6-Br-FAD}^{C}. The apparent first-order rate constant for flavinylation was 0.0028 s^{-1}, which is about $^1/_{10}$th the value of that for PchF{FAD} ($k = 0.025$ s^{-1}). We believe that this is the first example of an enzyme reconstituted with a 6-Br-flavin.

Free 6-Br-FAD has $\lambda_{max} = 401$ nm ($\epsilon = 11.7$ mM^{-1} cm^{-1}) and $\lambda_{max} = 449$ nm ($\epsilon = 9.2$ mM^{-1} cm^{-1}) (Figure 5A). For published data for 6-Br-Rbf (*11*), $\lambda_{max} = 397$ nm ($\epsilon = 12.5$ mM^{-1} cm^{-1}) and $\lambda_{max} = 445$ nm ($\epsilon = 9.7$ mM^{-1} cm^{-1}). For PchF{6-Br-FAD}^{NC} (Figure 5B), these two peaks merge to give a maximum at 408 nm and a shoulder around 450 nm. For PchF{6-Br-FAD}^{C}, the shoulder acquires some fine structure attributed to vibrational mode transitions.

The dithionite titrations of 6-Br-FAD, PchF{6-Br-FAD}^{NC}, and PchF{6-Br-FAD}^{C} are presented in Figures 5. The titration of PchF{6-Br-FAD}^{C} indicated the intermediate formation of a flavin radical, which has spectral properties reminiscent of an anionic radical ($\lambda_{max} \approx 385$ nm).

The $E_{m,7} = -165$ mV for free 6-Br-FAD is lower than the -149 mV found for 6-Br-Rbf by dithionite reduction in the presence of dyes (*11*). The determination of the 2-electron potential for PchF{6-Br-FAD}^{C} was complicated by the intermediate formation of the stable flavin radical. In this case, direct reduction of the dye indigotetrasulfonate by dithiothreitol (DTT) was used (*26*), without the presence of xanthine, xanthine oxidase, and methyl viologen. The reduced dye transfers 2 electrons to proteins without the generation of radicals (*26*). With this procedure, we found that $E_{m,7} = -48$ mV for PchF{6-Br-FAD}^{C}. Using the same dye, in conjunction with the xanthine/xanthine oxidase method, after correction for the presence of the radical, a value of -59 mV was determined. However, a straight line for the plot of $\ln(\text{protein}_{ox}/\text{protein}_{red})$ vs $\ln(\text{dye}_{ox}/\text{dye}_{red})$, with slope ~1, was obtained in a restricted interval; hence, we believe that the data obtained using DTT as the reductant are more reliable.

A factor analysis of dithionite titration data for PchF{6-Br-FAD}^{C} indicated that the maximal concentration of radical was 86%, which corresponds to the difference of +129 mV between the first and the second 1-electron redox potentials, $E_1 - E_2$ (vide supra). Therefore, $E_1 = -48 + 129/2 = +17$ mV, and $E_2 = -48 - 129/2 = -113$ mV.

PCMH{6-Br-FAD}^{C}. Since a limited amount of PchF{6-Br-FAD}^{C} was obtained, a small quantity of PCMH{6-Br-

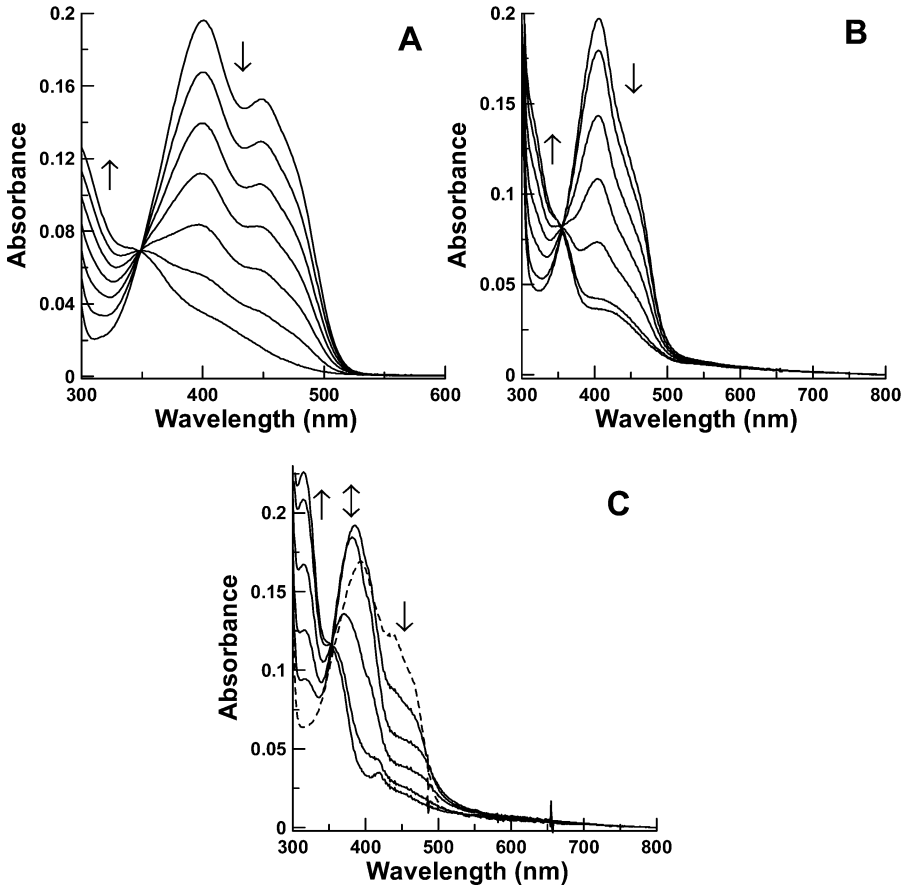

FIGURE 5: Anaerobic dithionite titrations of 6-Br-FAD, PchF{6-Br-FAD}^{NC}, and PchF{6-Br-FAD}^{C}. Frame A shows the dithionite titration of 16.3 μM 6-Br-FAD in 25 mM KH_2PO_4/KOH, pH 7.0 at 25 °C. The cumulative concentrations of added dithionite were 0, 2.70, 5.40, 8.08, 10.8, 13.4, and 16.1 μM. Frame B shows the dithionite titration of 12.7 μM PchF{6-Br-FAD}^{NC} in 25 mM KH_2PO_4/KOH, pH 7.0 at 25 °C. The cumulative concentrations of added dithionite were 0, 1.33, 3.99, 6.63, 9.27, 11.9, and 14.5 μM. Frame C shows the dithionite titration of 12 μM PchF{6-NH_2-FAD}^{NC} in 25 mM KH_2PO_4/KOH, pH 7.0 at 25 °C. The cumulative concentrations of added dithionite were 0, 3.14, 6.28, 9.40, 12.5, and 15.6 μM. The dashed line is the spectrum of the fully oxidized protein. In all frames, the arrows indicated the changes that occurred as progressively more dithionite was added. The double-headed arrow in frame C indicates that the absorbance in the 380−390 nm region first increases and then decreases, which suggests the formation and then disappearance of a flavin radical as the titration proceeds.

FAD}^{C} was produced by mixing the flavoprotein with PchC. This provided enough material for steady-state kinetic assays, a spectrum of the 4-Br-phenol−protein complex, and the measurement of the redox potential (Table 1).

PchF{8-Cl-FAD}^{NC}. The spectrum of free 8-Cl-FAD (ϵ_{448} = 11.6 mM^{-1} cm^{-1}) was identical to that reported by others (*27*). The redox potential of free 8-Cl-FAD was −152 mV (reference dye, indigo disulfonate), in agreement with the published value (*28*). The $E_{m,7}$(8-Cl-FAD) for PchF{8-Cl-FAD}^{NC} was found to be +16 mV.

The spectrum of PchF{8-Cl-FAD}^{NC} had λ_{max} = 435 nm (ϵ = 14 mM^{-1} cm^{-1}). Since 8-Cl-FAD lacks an 8-methyl group, it cannot bind covalently to PchF in the normal fashion. In addition, covalent flavinylation did not occur by elimination of Cl^- by the phenolate oxygen of Tyr384 or other protein-bound nucleophiles. Figure 6 shows the dithionite titration of PchF{8-Cl-FAD}^{NC}. The increase of the absorption at 385 nm indicated the formation of the (presumably anionic) flavin radical, which reaches almost 100% after addition of 1 electron equivalent, as determined by a factor analysis of the spectral data.

The 4-hydroxybenzyl alcohol titration of PchF{8-Cl-FAD}^{NC} proceeded in the same manner as that for PchF{8-Cl-FAD}^{NC} (vide infra). A factor analysis of the spectral data indicated the participation of three spectral species. By analogy with substrate titrations for other forms of PchF (vide supra and Figure S2) (*3*, *15*), it was concluded that these species are the oxidized protein spectrum, a hybrid spectrum due to the absorbances of the reduced protein and the oxidized protein−aldehyde complex, and the combined spectra of fully reduced protein and unbound aldehyde.

PCMH{8-Cl-FAD}^{NC}. Because a limited amount of 8-Cl-FAD was obtained, only a small amount of PchF{8-Cl-FAD}^{NC} could be produced. From this, enough PCMH{8-Cl-FAD}^{NC} was prepared to do steady-state kinetic studies, obtain the spectrum of the 4-Br-phenol−PchF{8-Cl-FAD}^{NC} spectrum, and measure the redox potential (Table 1).

PchF[Y384F]{8-Cl-FAD}^{NC}. As reported earlier (*6*), PchF[Y384F]{FAD}^{NC} has redox properties that are different from those of PchF{FAD}^{NC} or PchF{FAD}^{C}. The $E_{m,7}$ = +2 mV for PchF[Y384F]{FAD}^{NC} is higher than $E_{m,7}$ = −15 mV for PchF^{NC}. Therefore, we expected also to see a change in the redox properties of PchF[Y384F]{8-Cl-FAD}^{NC} relative to PchF[Y384F]{FAD}^{NC}. The $E_{m,7}$ value for the flavin bound to PchF[Y384F]{8-Cl-FAD}^{NC} was about +60 mV (Table 1). This is about 45 mV more positive than the potential of PchF{8-Cl-FAD}^{NC}, and 60 mV higher than the potential of PchF[Y384F]{FAD}^{NC}, but is about the same

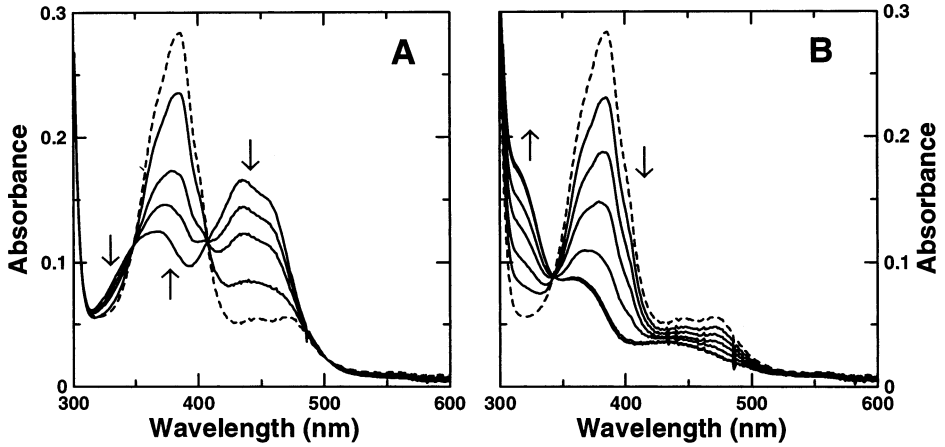

FIGURE 6: Anaerobic dithionite titration of PchF{8-Cl-FAD}^{NC}. This protein, 13.7 μM, was titrated in 25 mM KH_2PO_4/KOH, pH 7.0 at 25 °C. In both frames, the arrows indicated the changes that occurred as progressively more dithionite was added. Frame A shows the first part of the titration where a large increase in absorbance at 385 nm occurred. This indicated the formation of a substantial amount of the flavin radical. The dashed line is the spectrum for the maximum amount of radical that was generated. The cumulative concentrations of added dithionite were 0, 1.57, 3.12, 4.66, and 6.19 μM. Frame B shows the second phase of the titration. The dashed line is the same spectrum as that shown in frame A. The cumulative concentrations of added dithionite were 6.19, 7.71, 9.22, 10.7, 12.2, 13.7, and 15.2 μM.

as the potential of covalently bound FAD in PchF^{C}.

The spectral properties of PchF[Y384F]{8-Cl-FAD}^{NC} and the course of an anaerobic titration with dithionite were very similar to that for PchF{8-Cl-FAD}^{NC} (vide supra; Figure 6). The (apparently anionic) radical was observed after addition of first 0.5 electron equivalent. Interestingly, stable radicals were not generated during dithionite titrations of PchF{FAD}^{NC} and PchF[Y384F]{FAD}^{NC}.

The results of the reductive titration of PchF[Y384F]{8-Cl-FAD}^{NC} with 4-hydroxybenzyl alcohol are displayed in Figure S5 (Supporting Information). A factor analysis indicated that three spectral components were involved in the transformation from the oxidized to the reduced protein; the three components were the oxidized protein spectrum, the hybrid spectrum of the reduced protein plus oxidized protein−4-hydroxybenzaldehyde complex, and the composite spectrum of the fully reduced enzyme and the free aldehyde. The intermediate hybrid spectrum showed a weak CT band absorbing from 500 to 800 nm, with a λ_{max} at about 580 nm. This spectrum displayed also a large peak with λ_{max} = 435 nm, which, by analogy with the 4-hydroxybenzyl alcohol titration of other forms of PchF (vide supra and Figure S2) (*3*, *15*), is presumed to be due to the quinone methide-like tautomer of the bound aldehyde.

PCMH[Y384F]{8-Cl-FAD}^{NC}. The midpoint potential of flavin in PCMH[Y384F]{8-Cl-FAD}^{NC} was +104 mV. This value is 17 mV more positive than the $E_{m,7}$ value for unmodified FAD bound to normal PCMH.

DISCUSSION

Covalent Flavinylation. It was discovered that covalent flavinylation occurred for PchF{6-Br-FAD}^{NC} and PchF{6-NH_2-FAD}^{NC} on their exposure to PchC. This process produced a reduced covalently bound flavin, which was oxidized subsequently via electron transfers to an external acceptor with the heme of PchC as the conduit (Figure 1). Ours are the first example of in vitro covalent tethering of modified forms of FAD to a flavoprotein, although human monoamine oxidases A and B with covalently bound modified FAD were produced by a Rbf-deficient yeast expression system (*29*).

Precipitation of PchF{6-Br-FAD}^{C} or PchF{6-NH_2-FAD}^{C} with trichloroacetic acid and centrifugation yielded yellow- and green-colored denatured protein pellets, respectively, but free flavin in solution was not detected in either case. This proves conclusively that the flavins are bound covalently (*24*). Although peptide or mass spectral analyses were not done, by analogy with other forms of PchF and FAD, we are confident that 6-Br-FAD and 6-NH_2-FAD are attached covalently via their 8α-methylene to the phenolic oxygen of Tyr384 (*2*, *15*). For all of the forms of PchF with covalently bound FAD forms, the covalent bonds remained intact after the flavin was reduced. This contrasts with protein-free 8α-*O*-tyrosylriboflavin, which undergoes reductive cleavage to produce oxidized riboflavin and free tyrosine (*2*).

The rate of *p*-cresol oxidation by each PchF{X}^{C} form (X is FAD or modified FAD) was much faster than for the corresponding PchF{X}^{NC} form (Table 1). It was found also that the oxidation rate for PCMH{6-NH_2}^{C} was faster than PCMH{6-NH_2}^{NC} (Table 1). In addition, the rate constant for PCMH{X}^{C} substrate oxidation was higher than for the corresponding PchF{X}^{C} form (Table 1). These results indicate that the changes induced on association of PchF and PchC have a profound effect on catalysis. Furthermore, the k_{cat} values are seen to increase as the 2-electron potential increases (Table 1). However, the correlation is not straightforward because the catalytic efficiency depends also on the redox properties of *p*-cresol bound to each altered form of PchF and PCMH (*15*). The analysis, interpretation, and discussion of this phenomenon are presented in detail elsewhere (*19*). Interestingly, the lack of a covalent bond in some forms of PCMH did not prevent efficient electron transfer from the reduced flavin to the oxidized heme of PchC.

While 5-deaza-FAD has an 8-methyl group, it did not bind covalently when PchF{5-deaza-FAD}^{NC} was mixed with PchC. This suggests that the low electrophilicity of 5-deaza-FAD (as reflected by its low $E_{m,7}$) raises the pK_a of the proton on the 8-methyl group, thus thwarting the formation of the requisite iminoquinone methide-like intermediate (Figure 1). However, the 2-electron $E_{m,7}$ for the flavin of PCMH{5-

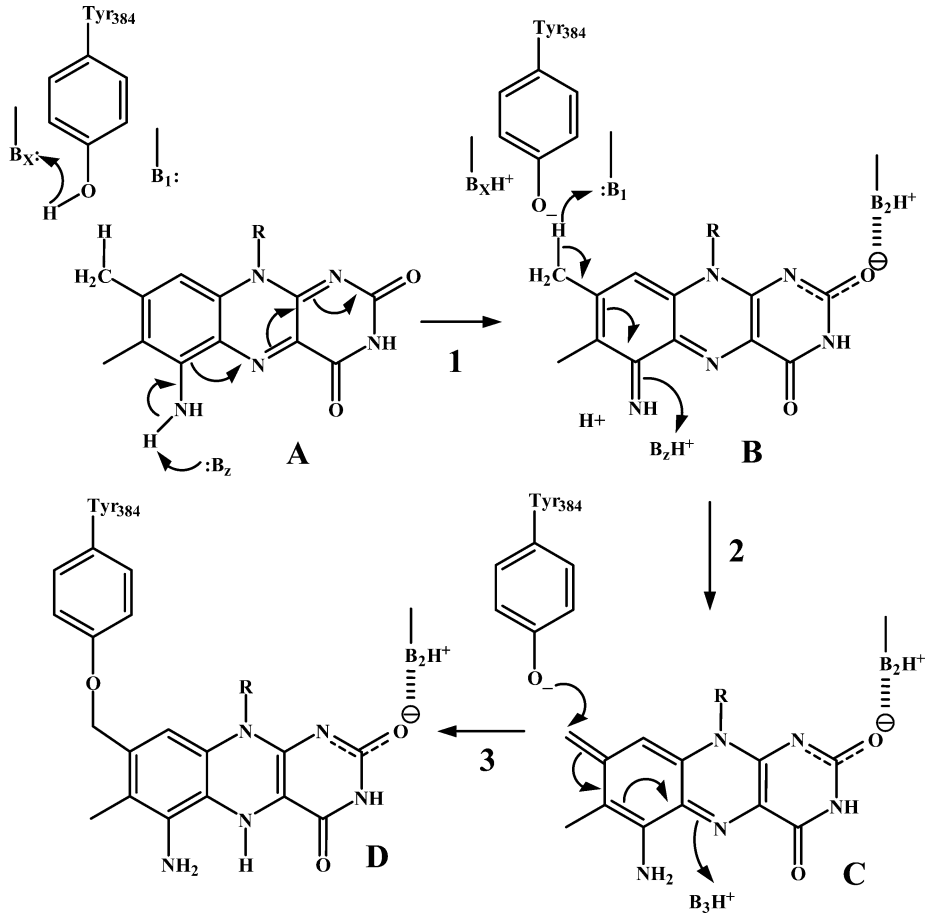

FIGURE 7: Proposed mechanism for the covalent flavinylation of PchF in PCMH{6-NH_2}^{NC}. See the legend to Figure 1 for the definitions of B_1, B_2, B_x, and R. B_z is a base that removes a proton from the 6-amino group. Step 3 produces reduced 6-NH_2-FAD, which is oxidized by the normal route via two 1-electron transfers to PchC (see Figure 1).

deaza-FAD}^{NC} is +16 mV, which is, astoundingly, about 300 mV more positive than the unassociated flavin (−311 mV for 5-deaza-Rbf and −278 mV for 5-deaza-FMN). If a high potential alone were the determining factor, we would expect that the flavin would become covalently bound for PCMH{5-deaza-FAD}^{NC}. We are at a loss to explain the large shift in the $E_{m,7}$ value of bound 5-deaza-FAD.

In contrast, the $E_{m,7}$ of the free form of 6-NH_2-FAD (−298 mV) increased slightly to −278 mV when it bound non-covalently to apo-PchF and increased further by 91 mV to −187 mV when PchF{6-NH_2-FAD}^{NC} complexed with PchC. However, covalent flavinylation of PCMH{6-NH_2-FAD}^{NC} did occur, albeit very slowly. Perhaps the flavin ring system can tautomerize to an electrophilic *p*-iminoquinone methide-like intermediate, which would be attacked at its 8-carbon by the phenolate oxygen of Tyr384 (Figure 7). A *p*-iminoquinone methide-type intermediate for bound 5-deaza-FAD could not form by this route.

Perhaps the potential of the flavin in the cytochrome-free form of PchF^{NC} determines if and how fast covalent flavinylation occurs. For PchF{FAD}^{NC} and PchF{6-Br-FAD}^{NC}, with high $E_{m,7}$(FAD) values of +87 and +63 mV, respectively, the covalent flavinylation rate is quite high. However, for PchF{6-NH_2-FAD}^{NC} ($E_{m,7}$ = −275 mV) and PchF{5-deaza-FAD}^{NC} ($E_{m,7}$ = −300 mV), the rate is very slow and apparently zero, respectively. We envision that PchF^{NC} and PchC form a weak complex and then (concerted?) conformational changes of both subunits and covalent flavinylation take place to give the mature, stable, tightly associated flavocytochrome complex. We speculate further that the initial weak interaction has little or a similar effect on the redox potentials (electrophilicity) of the flavins. Clearly, there remain aspects of this reaction to be explored.

PchF−4-Hydroxybenzaldehyde Complex. It was found that the redox potential of FAD bound to PchF was altered when 4-hydroxybenzaldehyde was bound. This explains the apparent biphasic changes observed during a *p*-cresol or a 4-hydroxybenzyl alcohol titration of various forms of holo-PchF, where the aldehyde is the final oxidation product (vide supra) (*3*, *15*). For the PchF{FAD}^{C}−aldehyde complex, K_D = 0.53 μM (*3*), and $E_{m,7}$ = +1 mV (reference dye, gallocyanine), which is 61 mV more negative than the potential for aldehyde-free PchF{FAD}^{C} (*6*). Thus, $K_D^{red} = K_D^{ox}$ exp(61 × 2/25.6) = 120 μM. As a result, during substrate titrations, the aldehyde that formed detaches from the reduced protein and then rebinds to the available oxidized form. For the 4-hydroxybenzyl alcohol titration of PchF^{C}, this was manifested spectrally by the intermediate appearance of a high-absorbing peak at 342 nm that is due to a quinone methide-like form of the bound aldehyde (Figure 8) (*3*). There appeared simultaneously a CT band in the 600 nm region. These features are superimposed on the spectrum of the fully reduced aldehyde-free protein. Since each addition of the alcohol produces an equivalent amount of PchF{FAD}$^{C}_{ox}$−aldehyde and PchF{FAD}$^{C}_{red}$, after the addition of half an equivalent of the alcohol, these two forms

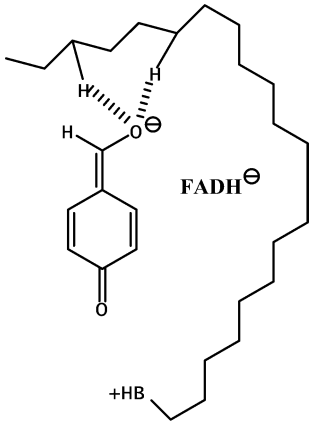

FIGURE 8: Proposed structure of 4-hydroxybenzaldehyde when bound to the reduced forms of PChF or PCMH. This structure of the anionic quinone methide-type form of the aldehyde bound to PchF or PCMH was deduced as described in a prior report (*3*). This species has a very intense, relatively narrow absorbance peak at 342 nm. Also shown is the fully reduced anionic form of FAD, i.e., $FADH^-$.

are present at equimolar concentrations. For the factor analysis of the titration data, the [PchF{FAD}$^{C}_{ox}$−aldehyde + PchF{FAD}$^{C}_{red}$]−hybrid spectrum was treated as if it were due to a unique component; the analysis indicated the participation of three spectral species: that for oxidized protein, that for fully reduced protein plus free aldehyde, and that for the hybrid.

We titrated the PchF{FAD}$^{C}_{ox}$−aldehyde complex with sodium dithionite. After addition of 1 electron equivalent, the maximum amount of the FAD radical formed; apparently, the aldehyde does not bind to the 1-electron-reduced protein, because as the radical forms, the 342 nm peak and the CT band decreased proportionally with the increase of an absorbance around 320 nm for free aldehyde. At the end of the titration, we saw the same spectrum that was observed at the completion of the 4-hydroxybenzyl alcohol titration.

A negative shift of redox potential was seen also for the aldehyde complex with normal PCMH; for complexed and uncomplexed PCMH, $E_{m,7} = +25$ and $+87$ mV, respectively; hence, $K_D^{red} = K_D^{ox} \exp(62 \times 2/25.6) = 127K_D^{ox}$. This situation is advantageous, because it ensures for efficient enzyme operation; the product dissociates rapidly and completely from the active site of the FAD-reduced species to facilitate rapid turnover. The weaker binding of the aldehyde to the reduced forms of PchF or PCMH may be due to unfavorable electrostatic interactions between a bound anionic quinone methide-type tautomer of the aldehyde (*3*) and the anionic fully reduced flavin ($FADH^-$) (Figure 8). Such an interaction would not be present in the oxidized enzyme−aldehyde complex because the flavin ring is uncharged.

Charge-Transfer Interactions. It is interesting that the oxidation product 4-hydroxybenzaldehyde, the substrate mimic 4-Br-phenol, and, in some cases, *p*-cresol interact via CT complexes with the bound flavins of various forms of PCMH and PchF (work reported herein and references *3*, *6*, and *15*). 4-Br-phenol was chosen for this study because the size of the bromo group is similar to that of a methyl group, although the electronic properties of 4-Br-phenol are quite different from those of *p*-cresol.

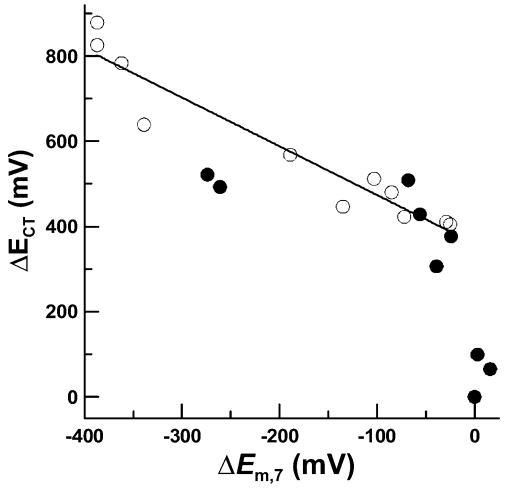

FIGURE 9: Plot of the ΔE_{CT} for the 4-Br-phenol CT band vs the $\Delta E_{m,7}$ for the FAD bound to each form of PchF/PCMH. $\Delta E_{CT} = E_{CT}$(protein) − E_{CT}(PCMH) and $\Delta E_{m,7} = E_{m,7}$(protein) − $E_{m,7}$(PCMH). $E_{CT} = h\nu_{CT} = hc/\lambda_{CT}$, where h = Planck's constant $= 4.1227 \times 10^{-15}$ eV·s and c = the speed of light $= 2.9979 \times 10^{17}$ nm/s. The open circles are for the PchF forms and the solid circles for the PCMH forms. The line represents the linear regression fit to the data represented by the open circles; slope $= -1.14 \pm 0.14$, intercept $= 359 \pm 27$ mV, and $R_2 = 0.918$.

The crystal structure of the PCMH−*p*-cresol complex (*1*) shows clearly a $\pi-\pi$ CT interaction between the substrate and the pyrazinoid/pyrimidinoid portions of the isoalloxazine system of FAD. The interaction is similar to those seen for model systems (*30*−*34*) and the structures of CT complexes between Old Yellow enzyme (OYE) and 4-hydroxybenzaldehyde (*36*), medium-chain acyl-CoA dehydrogenase and 3-thiaoctanoyl-CoA (*36*, *37*), 12-oxophytodienoate reductase and 9*S*,13*S*-12-oxophytodienoate (*38*), dihydroorotate dehydrogenase and orotate (*39*), D-amino acid oxidase and 4-aminobezoate (*40*), and sarcosine oxidase and pyrrole-2-carboxylate (*41*). Although we do not have the crystal structure of the PCMH−4-Br-phenol complex, because of the structural similarity of the 4-Br-phenol and *p*-cresol, we assume that the stereochemistry of the bound phenolate forms is the same for both (*1*).

For other flavoproteins (e.g., Old Yellow enzyme) (*42*), there exists a linear relationship between the energy, E_{CT}, for the bound substrate analogue, and the flavin's redox potential. A plot constructed from the E_{CT} (mV) and $E_{m,7}$ (mV) for data for the PchF and PCMH forms is displayed in Figure 9. Clearly, a simple (linear) correlation does not exist.

According to valence bond theory (*43*−*45*), $E_{CT} = h\nu_{CT} = I^D - E^A - W$, where I^D is the ionization potential of the donor, E^A is the electron affinity of the acceptor, and the work term, W, includes "no bond" interaction as well as the Coulombic attraction energy of the complex. Usually the value of W is small, and E^A and I^D values are derived from polarographic data (*43*). As with OYE, it is assumed that $E^A \approx E_1$, the 1-electron potential for the formation of the flavin semiquinone, or the 2-electron potential, $E_{m,7}$ (*9*, *42*). We assume also that the redox potential for *p*-cresol or 4-Br-phenol provides a good estimate for its I^D value (*46*). Hence, E_{CT} is a function of both E^A and I^D, but only the former can be measured in the form of $E_{m,7}$. However, the linear regression fit to the points for just the PchF forms gives a

slope of approximately 1 (1.14 ± 0.11) (Figure 9), which indicates that the I^D values for these proteins are nearly equal ($\Delta I^D \approx 0$).

Such a correlation does not seem to exist for the PCMH forms (the solid circles in Figure 9). However, the values of $E_{m,7}$ for the bound flavins were measured when the heme is reduced because the potential of the latter is always much more positive than the former. In contrast, E_{CT} values are for the interactions of 4-Br-phenol with oxidized flavins when the heme is also oxidized. Since there is a change in the charge of the heme iron from Fe^{3+} to Fe^{2+} when the heme becomes reduced, the electrostatic field impinging on the flavin could be different for PCMH with oxidized and reduced PchC. Since we presume that the radical and fully reduced forms of the bound flavins are anionic ($FAD^{\bullet -}$ and $FADH^-$), we predict that the $E_{m,7}$ value for the bound flavins would be higher when the heme is oxidized than when it is reduced. As a result, it is not possible to draw a global conclusion regarding the dependence of E_{CT} on the flavin's redox properties. For the purpose of further discussion (vide infra), we will assume that the $E_{m,7}$(flavin) values are similar when the heme is oxidized or reduced.

For PCMH, the value of $E_{m,7}$ for the covalently bound FAD is shifted by +30 mV with respect to unassociated PchF{FAD}^{C}. Since the flavin is the acceptor in a CT complex with 4-Br-phenol, assuming that I^D for this phenol is constant, one would predict a decrease of E_{CT} (i.e., a red-shifted absorbance maximum for CT band) upon association of PchC and PchF{FAD}^{C}. We found that the λ_{max} for the CT peak shifted from 655 nm for PchF{FAD}^{C} to 833 nm for PCMH{FAD}^{C}. The resulting small change in the amplitude of the CT band suggests that PchC interacts electrostatically only with PchF{FAD}^{C}. Hence, the overlap of the orbitals of the aromatic portions of FAD and 4-Br-phenol, which defines the shape and the amplitude of the band, is similar. The locations of the maxima are different because E^A and I^D are affected by the electrostatics of the system.

The shift from 655 to 833 nm corresponds to change in E_{CT} from 1.895 to 1.490 eV, i.e., a decrease of ~405 mV (=ΔE_{CT}). Since the contribution of the change in $\Delta E_{m,7}$(FAD)-(≈ΔE^A) to ΔE_{CT} is 27 mV, the remaining ~380 mV must be due to a decrease in I^D for 4-Br-phenol. However, $E_{m,7}$(FAD) may change when 4-Br-phenol binds, as occurs when 4-hydroxybenzaldehyde binds. We found that $E_{m,7}$ = +22 mV for the PchF{FAD}^{C}−4-Br-phenol complex, and it was +48 mV for the PCMH{FAD}^{C}−4-Br-phenol complex. The corresponding values without this phenol bound are +60 and +87 mV, respectively. Therefore, the presence of 4-Br-phenol decreases both potentials by approximately the same value of 27 mV, and therefore, ΔI^D is still ~380 mV.

Since *p*-cresol and 4-Br-phenol are assumed to interact with FAD of PCMH in a similar manner, we believe that $\Delta I^D_{p-cresol} \approx \Delta I^D_{4-Br-phenol}$ (*15*). The rate constant, *k*, can be expressed as $\exp[\alpha(E^A - I^D)/kT]$ ($\alpha = 0.3$, the symmetry factor or transfer coefficient, and *k* is the Boltzmann constant) (ref *15* and references cited therein). Hence, the rate enhancement for PCMH relative to PchF{FAD}^{C} would be about a factor $80 \approx \exp[0.3 \times 378\ mV/25.6\ mV]$. The k_{cat} values for PCMH and PchF{FAD}^{C} are 121 and 1 s^{-1}, respectively, or a 120-fold change. The remaining contribution comes from $\Delta E_{m,7}$(FAD) = +27 mV: $\exp[0.3 \times \{27\ mV - (-378\ mV)\}/25.6\ mV] \approx 115$-fold difference. More details concerning this issue can be found elsewhere (*19*).

From our studies, it is not clear if a *p*-cresol CT complex is an obligatory intermediate in the catalytic reaction. We only see CT complexes between *p*-cresol and PchF forms that have very low activity, e.g., PchF{FAD}^{NC} (*3*), PchF-{iso-FAD}^{NC}, and PchF(5-deaza-FAD}^{NC}. In fact, it is the low activities that allowed us to analyze the spectral properties in static nonreductive substrate titrations (vide supra) (*3*). In contrast, a CT complex was not detected during stopped-flow reactions of *p*-cresol or *p*-cresol-α,α,α-d_3 with PCMH (*17*), although, if such a complex did form, but did not accumulate to an appreciable extent, it would be difficult to detect because it has a small extinction coefficient. In addition, there would be interference from the absorbance of the heme in the spectral region where we might expect the complex to absorb. Further work (e.g., stopped-flow studies), possibly with other substrates, is necessary to establish if a CT complex between bound flavin and substrate is an obligatory catalytic intermediate.

If a CT complex is an intermediate in the PCMH reaction, what purpose does it serve? Some insight may be gleaned from the studies of acyl-CoA dehydrogenases. It has been proposed that the (CT) interaction of FAD and substrate for the mammalian medium-chain acyl-CoA dehydrogenase benefits catalysis; on abstraction of the substrate's α proton, the negative charge (ground-state CT) delocalizes into the isoalloxazine ring of FAD. This would be manifested in a lowering of the pK_a of the α proton and a stabilization of the transition state for dehydrogenation (*37*, *47*−*49*). It was suggested that this and other interactions of the substrate with the enzyme lower the pK_a to a value that allows the α proton to be removed by a carboxylate group (Glu376) of this enzyme (*37*, *47*).

In a similar fashion, a ground-state "CT" interaction in PCMH could lower the pK_a of *p*-cresol so that it is efficiently converted to the phenolate form after binding, which could facilitate catalysis (*50*). When bound to PCMH, the hydroxyl group of *p*-cresol is within hydrogen-bonding distance of the phenolate oxygens of Tyr95 and Tyr473 (*1*). Hence, either of these amino acyl groups could provide the base for removal of *p*-cresol's phenolic proton. For this scenario, in the Michealis complex, the hydroxyl group of a tyrosyl residue would be unprotonated, and its pK_a should be equal to or greater than that of phenolate proton of *p*-cresol complexed to FAD so that rapid substrate deprotonation would ensue. Work is in progress to elucidate this aspect of catalysis.

In summary, the work with 4-hydroxybenzaldehyde confirms our earlier conclusion that it and probably *p*-cresol bind as the phenolate forms (*3*). We also discovered that this aldhyde binds more avidly to oxidized forms of PchF and PCMH, and this has implications for efficient catalysis. Herein, we present also the first examples of modified flavins becoming covalently bound in vitro and that this process may depend on the redox potential of the noncovalently bound flavin analogue. Interestingly, even the very low potential and weakly electrophilic 6-NH_2-FAD became covalently bound to PchF{6-NH_2-FAD}^{NC} when this protein was exposed to PchC. This implies that the basic mechanism for this process is intact and it is quite robust. In addition, it

was discovered that the efficiency of *p*-cresol oxidation increased as the value of $E_{m,7}$ of the bound flavin increased, whether the potential increase was due to covalent flavinylation and/or association of PchC with various PchF forms. Furthermore, it was found that the energy of the 4-Br-phenol−flavin CT band, E_{CT}, increased as the $E_{m,7}$ of the bound flavin decreased. While there seemed to be a fairly good linear correlation between these parameters for the PchF forms (I^D for bound 4-Br-phenol is invariant), a global correlation was not apparent. We conclude that E_{CT} correlates with the redox properties of both the bound flavin (E^A) and bound substrate mimic, 4-Br-phenol (I^D). In addition, we only have $E_{m,7}$ values for PCMH when the heme is reduced, not when it is oxidized, which are required for this analysis. The correlations between redox properties, catalytic efficiency, and CT interaction and their connection are dealt with in great detail elsewhere (*19*).

In closing, our work has shed more light on several aspects of the mechanisms of covalent flavinylation and substrate oxidation and has provided guidance for future research in these areas.

SUPPORTING INFORMATION AVAILABLE

A scheme displaying the redox properties and reactions of PchF, PchC, and PCMH, spectral data for the titrations of several forms of PchF, and the plot used to determine $E_{m,7}$(iso-FAD) for PCMH{iso-FAD}^{NC}. This material is available free of charge via the Internet at http://pubs.acs.org.

REFERENCES

1. Cunane, L., Chen, Z. W., Shamala, N., Mathews, F. F., Cronin, C. N., and McIntire, W. S. (2000) Structures of the flavocytochrome *p*-cresol methylhydroxylase and its enzyme−substrate complex: Gated substrate entry and proton relays support the proposed catalytic mechanism, *J. Mol. Biol. 295*, 357−364.
2. McIntire, W. S., Edmondson, D. E., Hopper, D. J., and Singer, T. P. (1981) 8α-(*O*-Tyrosyl)flavin adenine dinucleotide, the prosthetic group of bacterial *p*-cresol methylhydroxylase, *Biochemistry 20*, 3068−3075.
3. Engst, S., Kuusk, V., Efimov, I., Cronin, C. N., and McIntire, W. S. (1999) Properties of *p*-cresol methylhydroxylase flavoprotein overproduced by *Escherichia coli*, *Biochemistry 38*, 16620−16628.
4. Kim, J., Fuller, J. H., Kuusk, V., Cunane, L., Chen, Z. W., Mathews, F. S., and McIntire, W. S. (1995) The cytochrome subunit is necessary for covalent FAD attachment to the flavoprotein subunit of *p*-cresol methylhydroxylase, *J. Biol. Chem. 270*, 31202−31209.
5. Koerber, S. C., McIntire, W. S., Bohmont, C., and Singer, T. P. (1985) Resolution of the flavocytochrome *p*-cresol methylhydroxylase into subunits and reconstitution of the enzyme, *Biochemistry 24*, 5276−5280.
6. Efimov, I., Cronin, C. N., and McIntire, W. S. (2001) Effects of noncovalent and covalent FAD binding on the redox and catalytic properties of *p*-cresol methylhydroxylase, *Biochemistry 40*, 2155−2166.
7. Koerber, S. C., Hopper, D. J., McIntire, W. S., and Singer, T. P. (1985) Formation and properties of flavoprotein-cytochrome hybrids by recombination of subunits from different species, *Biochem. J. 231*, 383−387.
8. Stankovich, M. T. (1991) Redox properties of flavins and flavoproteins, in *Chemistry and Biochemistry of Flavoenzymes* (Müller, F., Ed.) Vol. I, Chapter 18, pp 401−425, CRC Press, Boca Raton, FL.
9. Abramovitz, A. S., and Massey, V. (1976) Interaction of phenols with Old Yellow Enzyme. Physical evidence for charge-transfer complexes, *J. Biol. Chem. 251*, 5327−5336.
10. Hersh, L. B., and Walsh, C. (1980) Preparation, characterization, and coenzymic properties of 5-carba-5-deaza and 1-carba-1-deaza analogs of riboflavin, FMN, and FAD, *Methods Enzymol. 66*, 277−287.
11. Ghisla, S., Kenney, W. C., Knappe, W. R., Mcntire, W. S., and Singer, T. P. (1980) Chemical synthesis and some properties of 6-substituted flavins, *Biochemistry 19*, 2537−2544
12. Ghisla, S., and Massey, V. (1986) New flavins for old: Artificial flavins as active site probes of flavoproteins, *Biochem. J. 239*, 1−12.
13. Efimov, I., Kuusk, V., Zhang, X., and McIntire, W. S. (1998) Proposed steady-state kinetic mechanism for *Corynebacterium ammoniagenes* FAD synthetase produced by *Escherichia coli*, *Biochemistry 37*, 9716−9723.
14. Massey, V. (1991) A simple method for the determination of redox potentials, in *Flavins and Flavoproteins* (Curti, B., Ronchi, S., and Zanetti, G., Eds.) pp 59−66, Walter de Gruyter & Co., New York.
15. Efimov, I., Cronin, C. N., Bergmann, D. J., Kuusk, V., and McIntire, W. S. (2004) Insights into covalent flavinylation and catalysis from redox, spectral and kinetic analyses of the R474K mutant of the flavoprotein subunit of *p*-cresol methylhydroxylase, *Biochemistry 43*, 6138−6148.
16. Manstein, D. J., and Pai, E. F., (1986) Purification and characterization of FAD synthetase from *Brevibacterium ammoniagenes*, *J. Biol. Chem. 261*, 16169−16173.
17. McIntire, W. S., Hopper, D. J., and Singer, T. P. (1987) Steady-state and stopped-flow kinetic measurements of the primary deuterium isotope effect in the reaction catalyzed by *p*-cresol methylhydroxylase, *Biochemistry 26*, 4107−4117.
18. Edmondson, D. E., and Singer, T. P. (1973) Oxidation−reduction properties of the 8α-substituted flavins, *J. Biol. Chem. 248*, 8144−8149.
19. Efimov, I., and McIntire, W. S. (2004) The relationship between charge-transfer interactions, redox potentials and catalysis for different forms of the flavoprotein component of *p*-cresol methylhydroxylase, *J. Am. Chem. Soc.* (submitted for publication).
20. Choong, Y. S., and Massey, V. (1981) Studies on lactate oxidase substituted with synthetic flavins. Iso-FMN lactate oxidase, *J. Biol. Chem. 256*, 8671−8678.
21. Massey, V., Hemmerich, P., Knappe, W. R., Duchstein, H. J., and Fenner, H. (1978) Photoreduction of flavoproteins and other biological compounds catalyzed by deazaflavins, *Biochemistry 17*, 9−17.
22. Massey, V. (1994) Activation of molecular oxygen by flavins and flavoproteins, *J. Biol. Chem. 269*, 22459−22462.
23. McIntire, W. S., Hopper, D. J., and Singer, T. P. (1985) *p*-Cresol methylhydroxylase. Assay and general properties, *Biochem. J. 228*, 325−335.
24. Singer, T. P., and McIntire, W. S. (1984) Covalent attachment of flavin to flavoproteins: Occurrence, assay, and synthesis, *Methods Enzymol. 106*, 369−378.
25. Clark, W. M. (1972) *Oxidation−Reduction Potentials of Organic Systems*, Chapter 7, pp 184−203, Robert E. Kreiger Publishing Co., Huntington, NY.
26. Chaiyen, P., Brissette, P., Ballou, D. P., and Massey, V. (1997) Thermodynamics and reduction kinetics properties of 2-methyl-3-hydroxypyridine-5-carboxylic acid oxygenase, *Biochemistry 36*, 2612−2621.
27. Sucharitakul, J., Chaiyen, P., Ballou, D. P., and Massey, V. (2002) Probing the mechanism of 2-methyl-3-hydroxypyridine-5-carboxylic acid oxygenase by using 8-substituted-FAD analogs, in *Flavins and Flavoproteins* (Chapman, S. K., Perham, R. N., and Scrutton, N. S., Eds.) pp 381−386, Rudolf Weber, Agency for Scientific Publication, Berlin.
28. Ortiz-Maldonado, M., Ballou, D. P., and Massey, V. (1999) Use of free energy relationships to probe the individual steps of hydroxylation of *p*-hydroxybenzoate hydroxylase: Studies with a series of 8-substituted flavins, *Biochemistry 38*, 8124−8137.
29. Miller, J. R., and Edmondson, D. E. (1999) Influence of flavin analogue structure on the catalytic activities and flavinylation reactions of recombinant human liver monoamine oxidases A and B, *J. Biol. Chem. 274*, 23515−23525.
30. Breinlinger, E. C., Keenan, C. J., and Rotello, V. M. (1998) Modulation of flavin recognition and redox properties through donor atom−π interactions, *J. Am. Chem. Soc. 120*, 8606−8609.

31. Breinlinger, E. C., and Rotello, V. M. (1997) Model systems for flavoenzyme activity. Modulation of flavin redox potentials through π-stacking interactions, *J. Am. Chem. Soc. 119*, 1165−1166.
32. Goodman, A. J., Breinlinger, E. C., McIntosh, C. M., Grimaldi, L. N., and Rotello, V. M. (2001) Model systems for flavoenzyme activity. Control of flavin recognition via specific electrostatic interactions, *Org. Lett. 3*, 1531−1534.
33. Ishida, T., Itoh, M., Horiuchi, M., Yamashita, S., Doi, M., Inoue, M., Mizunoya, Y., Tona, Y., and Okada, A. (1986) Structural studies of the interaction between indole derivatives and biologically important aromatic compounds. Part XIV. On the interaction between flavin and indole rings. Crystallographic, spectroscopic, polarographic and energy calculational studies of a flavinyltryptamine peptide, *Chem. Pharm. Bull. 34*, 1853−1864.
34. Niemz, A., and Rotello, V. M. (1999) From enzyme to molecular device. Exploring the interdependence of redox and molecular recognition, *Acc. Chem. Res. 32*, 44−52.
35. Fox K. M., and Karplus, P. A. (1994) Old yellow Enzyme at 2-Å resolution: Overall structure, ligand binding, and comparison with related flavoproteins, *Structure 2*, 1089−1105.
36. Tomitsuka, E., Hirawake, H., Goto, Y., Taniwaki, M., Harada, S., and Kita, K. (2003) Direct evidence for two distinct forms of the flavoprotein subunit of human mitochondrial Complex II (succinate-ubiquinone reductase), *J. Biochem. (Tokyo) 134*, 191−195.
37. Nishina, Y., Sato, K., Tamaoki, H., Tanaka, T., Setoyama, C., Miura, R., and Shiga, K. (2003) Molecular Mechanism of the Drop in the pK_a of a Substrate Analog Bound to Medium-Chain Acyl-CoA Dehydrogenase: Implications for Substrate Activation, *J. Biochem. (Tokyo) 134*, 835−842.
38. Breithaupt, C., Strassner, J., Breitinger, U., Huber, R., Macheroux, P., Schaller, A., and Clausen, T. (2001) X-ray structure of 12-oxophytodienoate reductase 1 provides structural insight into substrate binding and specificity within the family of OYE, *Structure 9*, 419−429.
39. Rowland, P., Norager, S., Jensen, K. F., and Larsen, S. (2000) Structure of dihydroorotate dehydrogenase B: Electron transfer between two flavin groups bridged by an iron−sulfur cluster, *Structure 8*, 1227−1238.
40. Miura, R. (2001) Versatility and specificity in flavoenzymes: Control mechanisms of flavin reactivity, *Chem. Rec. 1*, 183−194.
41. Zhao, G., Song, H., Chen, Z. W., Mathews, F. S., and Schuman-Jorns, M. (2002) Monomeric sarcosine oxidase: Role of histidine 269 in catalysis, *Biochemistry 41*, 9751−9764.
42. Massey, V., Meah, Y., Xu, D., and Brown, B. J. (1999) New things about old yellow enzyme, in *Flavins and Flavoproteins* (Ghisla, S., Kroneck, P, Macheroux, P., and Sund, H., Eds.) pp 645−653, Rudolf Weber, Agency for Scientific Publication, Berlin.
43. Foster, R. (1969) *Organic Charge Transfer Complexes*, Chapters 2 and 3, pp 18−93, Academic Press, London and New York.
44. Murrell, J. N., Kettle, S. F. A., and Tedder, J. M. (1965) *Valence Theory*, 2nd ed., Chapter 18, pp 358−363, John Wiley & Sons, New York.
45. Gutmann, F., Johnson, C., Keyser, H., and Molnár, J. (1997) *Charge Transfer Complexes in Biological Systems*, Chapter 1, pp 1−12, Marcel Dekker, New York.
46. Rosokho, S. V., and Kochi, J. K. (2001) Mechanism of inner-sphere electron transfer via charge-transfer (precursor) complexes. Redox energetics of aromatic donors with the nitrosonium acceptor, *J. Am. Chem. Soc. 123*, 8985−8999.
47. Dmitrenko, O., Thorpe, C., and Bach, R. D. (2003) Effect of a charge-transfer interaction on the catalytic activity of acyl-CoA dehydrogenase: A theoretical study of the role of oxidized flavin, *J. Phys. Chem. B 107*, 13229−13236.
48. Ghilsa, S., and Thorpe, C. (2004) Acyl-CoA dehydrogenases. A mechanistic overview, *Eur. J. Biochem. 271*, 494−508.
49. Satoh, A., Nakajima, Y., Miyahara, I., Hirotsu, K., Tanaka, T., Nishina, Y., Shiga, K., Tamaoki, H., Setoyama, C., and Miura, R. (2003) Structure of the transition state analog of medium-chain acyl-CoA dehydrogenase. Crystallographic and molecular orbital studies on the charge-transfer complex of medium-chain acyl-CoA dehydrogenase with 3-thiaoctanoyl-CoA, *J. Biochem. (Tokyo) 134*, 297−304.
50. McIntire, W. S., Everhart, E. T., Craig, J. C., and Kuusk, V. (1999) A new procedure for deconvolution of inter-/intramolecular intrinsic primary and α-secondary deuterium isotope effects from enzyme steady-state kinetic data, *J. Am. Chem. Soc. 121*, 5865−5880.

BI049375D